# Strategies for Joint Radar-Communication Spectrum Sharing

Ammar Ahmed

Advisor: Dr. Yimin D. Zhang

Dissertation Proposal

Presented to

the Faculty of Temple University

November 2019

Disclaimer: Some parts of this document contain the contents from published or submitted articles of the author.

# Abstract

Spectrum sharing has become increasingly important since the past decade due to ongoing congestion of spectral resources. Higher data rates in wireless communications require the expansion of existing frequency allocations. Moreover, the technical advances which bene t end consumers demand new allocation of spectral resources. Signi cant research e orts have been made in the direction of cognitive radio in order to e ectively manage the existing frequency usage. Recently, coexistence of multiple platforms within same frequency bands has molli ed the spectral congestion by simultaneously sharing the same spectral resources for multiple applications.

The coexistence of radar and communication platforms in the same frequency bands will require both systems to work collaboratively in order to mitigate their mutual interference. This challenge can be signi cantly simpli ed if both systems are controlled by a joint control entity. Joint radar-communication (JRC) system is such an example where radar and communication system objectives are achieved by the same physical platform. JRC systems exploit either sensor array based beamforming or a single transmit antenna. In this research proposal, we discuss the research objectives we have accomplished so far as well as the future research directions related to JRC spectrum sharing.

We propose a QAM based sidelobe modulation scheme for beamforming based JRC systems which enhances the communication data rate by enabling multiple access strategy. The main principle of this proposed strategy lies in the capability of the beamformer to allow distinct amplitudes and phases in di erent directions. We also published work related to the optimal power allocation for such a spectrum sharing approach by employing spatial power control based beamforming approach.

Our second main contribution is the distributed JRC, which is the rst e ort in this research direction, enabling spectrum sharing for networked radar systems coexisting with the communication systems. We also devised a power allocation

strategy for such a system by employing convex optimization. For this purpose, the target localization error and the Shannon capacity are respectively considered to be the optimization criteria for radar and communication systems.

Our future research work will investigate the optimal sensor selection for beamforming based JRC systems. Such sensor selection strategies have become an increasingly interesting topic as the sensors become signi cantly cheaper and smaller relative to the hardware up-conversion chains. In this context, we will investigate the applicability of modern sparse regression based approaches.

# Contents

# List of Tables

# List of Figures

# Chapter 1

# Introduction

Spectrum sharing has recently gained a signi cant research attention due to the ongoing congestion of wireless spectrum caused by the broadband wireless communications and ever-increasing deployment of new applications aiming to consume the same spectral resources [1{4]. Modern wireless communication systems require immense expansion of existing spectral allocations in order to achieve high data rates to ensure the success of future generations of wireless systems. Moreover, new technical advancements and emerging applications which bring various advantages to the end users require new allocations of frequency resources [5]. In this context, great e orts have been invested in the eld of cognitive radios to improve the spectral e ciency so as to e ectively manage the existing usage of electromagnetic spectrum [6].

Recently, the problem of spectral competition between radar and communication systems has been addressed by coexistence or joint transmission based schemes. The coexistence of radar and communication platforms in the same frequency bands, requires both systems to work collaboratively in order to mitigate the mutual interference [7{15]. On the other hand, the strategies enabling joint transmission, like joint radar-communication (JRC) systems, perform the secondary communication op-

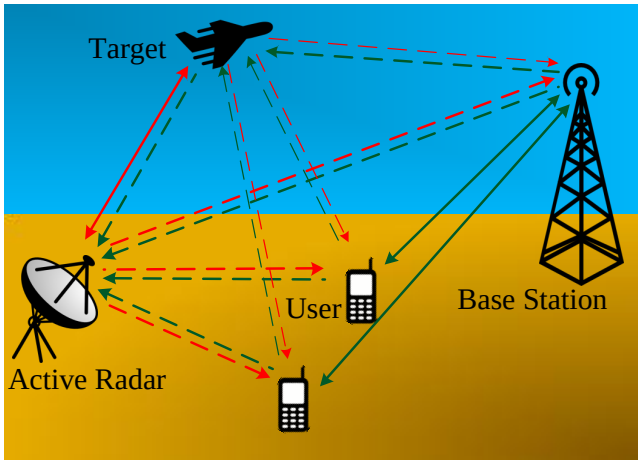


(a) Coexistence of radar and communication systems

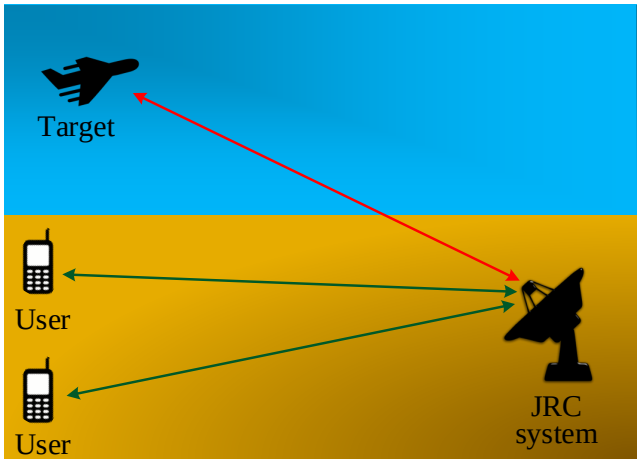


(b) Single transmitter based joint radar-communication system

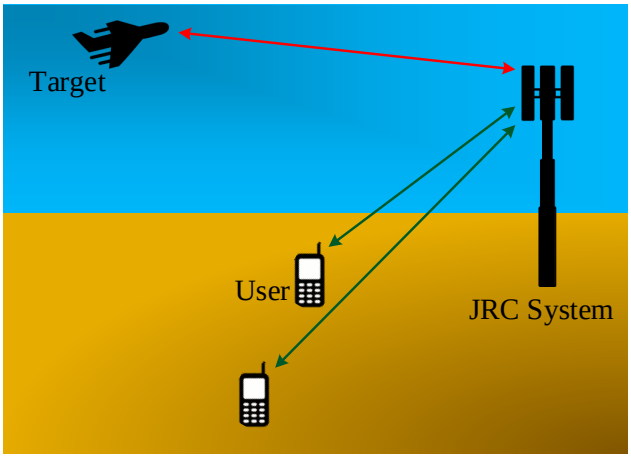


(c) Beamforming based joint radar-communication system

Figure 1.1: Existing radar-communication spectrum sharing strategies

eration in addition to the primary radar function while utilizing the same spectral resources [16{31].

Fig. 1.1 shows three di erent scenarios of spectrum sharing. Fig. 1.1(a) illustrates the coexistence of radar and communication systems within same spectral bands resulting in mutual interference between the two systems. Several research e orts have been made in the direction of space division multiplexing and transmit waveform design to mollify the mutual interference problem for coexisting radar and communication systems [11, 12]. Fig. 1.1(b) illustrates the JRC system where a joint transmission based strategy is used to perform radar as well as communication operation. Unlike coexistence, the transmission of electromagnetic waves can be controlled by the same physical entity which performs both tasks. Fig. 1.1(c) shows beamforming based JRC system. Such system are more exible than the single transmitter based systems as they are capable to transmit di erent signals in di erent directions due to their spatial multiplexing capabilities.

In this dissertation, we only focus on the spectrum sharing strategies for JRC transmission. The basic principle of a JRC system is to transmit waveforms for achieving radar and communication objectives by using the same physical platform as illustrated in Fig. 1.1. JRC systems achieve their objectives either by spatially multiplexing the signal transmission using smart antenna arrays [7, 19, 20, 22, 31{39], or by employing waveform diversity [1, 17, 18, 40{45], or both. The communication operation is realized by either embedding the communication information in the radar waveform or by dedicating separate waveforms for radar and communication operation [1, 4, 7, 13, 17{20, 22, 31, 33{45]. Important objectives of a radar system considered in such work are the maximization of transmit energy in the direction of targets. Communication objectives are considered to be secondary and focus on the bit error rate minimization of the communication receivers.

In the following, we discuss the existing work on JRC systems. Our most of the focus throughout this proposal is on beamforming based JRC systems.

## 1.1 Beamforming based JRC System

In beamforming based JRC systems, a sensor array is exploited to steer radar and communication signals in di erent directions. The waveforms for both radar and communication operations are transmitted from the same physical antenna array. In this case, communication is considered to be the secondary objective of the JRC system and is enabled by embedding information in the radar waveforms such that the primary radar operation is not compromised.

Fig. 1.1(c) shows the basic principle of beamforming based JRC system. The notable techniques in this research direction include the sidelobe control methods based on amplitude modulation (AM) [20], multi-waveform amplitude shift keying (ASK) [21{23], and phase shift keying (PSK) [24{26]. The sidelobe AM method [20] exploits multiple beamforming weight vectors corresponding to di erent sidelobe levels at the communication receivers located in the sidelobe region of radar. Each sidelobe level is mapped to a unique communication symbol. In the multi-waveform ASK based method [21], multiple orthogonal radar waveforms are employed such that each waveform is transmitted by one of the two beamformers implementing two di erent sidelobe levels. The communication receiver decodes the transmitted information by matched ltering the received waveform and extracting the sidelobe level information.

Although, the aforementioned ASK based method exploits waveform diversity, only two sidelobe levels are utilized. The method in [23] increases the e ective signal-to-noise ratio (SNR) at the communication receivers by using only one beamforming weight vector corresponding to the maximum allowable sidelobe level. Unfortunately,

all the ASK based methods discussed above can only broadcast the same communication information to all the communication users.

In PSK based JRC methods [24{26], information embedding is achieved by a dictionary of beamforming weight vectors having the same beampattern but di erent phase response towards the communication receivers. The communication receivers detect the corresponding phase symbols embedded in the received radar waveforms to determine the transmitted information either by coherent demodulation or with the help of a reference radar waveform transmitted through a reference beamfoming weight vector. However, the PSK based method cannot exploit the exibility of having di erent sidelobe levels.

### 1.1.1 Signal Model

Consider a JRC system equipped with an $M$-element transmit antenna array of an arbitrary con guration. Let $P$ denote the total power transmitted by the antenna array during each radar pulse, and $f\ _1(t);\ _2(t);:::;\ _{\hat{K}}(t)g$ be the $\hat{K}$ possible radar waveforms orthogonal to each other such that:

$$\frac{1}{T}\int_0^T\ _{k_1}(t)\ \ _{k_2}(t)\mathrm{d}t = \ (k_1\ \ k_2);\quad 1\ \ k_1;k_2\ \ \hat{K}; \tag{1.1}$$

where $t$ is the fast time, $T$ is the time duration of each radar pulse, $k_1$ and $k_2$ are positive integers, and ( ) is the Kronecker delta function.

The objective of existing sidelobe control based JRC schemes is to send information symbols to the communication receivers located in the sidelobe region without introducing perturbation to the primary radar operation [19{28]. This implies that the average transmit power of the radar waveform must not vary during each transmitted pulse. In order to realize this objective, ASK based schemes exploit di erent beamforming vectors to transmit di erent sidelobe levels in the directions of com-

munication receivers while keeping the radar's main beam at a constant amplitude. On the other hand, PSK based schemes rely on the transmission of di erent phases towards the communication receivers during each radar pulse such that the amplitude levels towards the communication receivers and the radar's main beam are not perturbed.

### 1.1.2 Beamforming Weight Vector Design

The following optimization can be used to synthesize the beamforming weight vectors for JRC schemes [19, 22{26]:

$$\begin{aligned} &\min_{\mathbf{w}_l} \max_{m} \; e^{j\,'(\ _m)} \quad \mathbf{w}_l^{\mathrm{H}}\mathbf{a}(\ _m) \;; \quad \ _m \ 2 \quad ; \\ &\text{subject to} \quad \mathbf{w}_l^{\mathrm{H}}\mathbf{a}(\ _p) \quad \text{"}; \quad \ _p \ 2 \quad ; \\ &\qquad\qquad \mathbf{w}_l^{\mathrm{H}}\mathbf{a}(\ _r) = \ _l; \quad 1 \quad l \quad L; 1 \quad r \quad R: \end{aligned} \tag{1.2}$$

Here, is the set of angles at which the radar main beam (main lobe) operates, is the complement set of representing the sidelobe region, $\mathbf{a}(\ )$ is the response vector of the transmitting antenna array at the angle , $'(\ )$ is the phase pro le of user's choice, $\mathbf{w}_l$ is the desired beamforming vector which achieves the sidelobe level $_l$ at all the communication receivers located at angles $_r \ 2$ , $R$ is the total number of communication receivers located in the sidelobe region, $L$ denotes the total number of allowable sidelobe levels, and $(\ )^{\mathrm{H}}$ represents the Hermitian transpose operator.

In the following, we summarize the sidelobe control based JRC schemes [19{28].

### 1.1.3 ASK Based Schemes

The information embedding in the radar waveform by exploiting ASK based techniques [19{23] can be realized by projecting varying sidelobe levels towards the directions of communication receivers located in the sidelobe region of the radar. These

sidelobe levels change from one pulse to other but remain constant during the course of each radar pulse. We can generate $L$ beamforming weight vectors by using the optimization in Eq. (1.2) such that each vector results in a unique sidelobe level $_l$ in the directions of communication receivers. If one radar waveform is exploited, the signal transmitted from the JRC platform during one radar pulse using one of the $L$ available beampatterns can be expressed as follows [19, 20]:

$$s(t; ) = \sqrt{\frac{P}{K}} \sum_{l=1}^{K} b_l( ) w_{l \quad k}(t); \tag{1.3}$$

where is the slow time (i.e., pulse index)[1], $_k(t)$ is the arbitrary waveform selected from $K$ possible radar waveforms, $b_l( )$ is the binary selection coefficient such that $\sum_{l=1}^{L} b_l( ) = 1$ for each radar pulse, $P$ is the transmit power of the radar, and $(:)$ denotes the conjugate operator.

Multiple orthogonal radar waveforms can be exploited to improve the detection performance of radar and increase the information rate of communication [19, 21{23]. In [21, 22], $K$( $K$) orthogonal radar waveforms are utilized and the transmitted signal vector for this scheme is given as:

$$s(t; ) = \sqrt{\frac{P}{K}} \sum_{k=1}^{K} b_k( ) w_{\text{low}} + (1 \quad b_k( )) w_{\text{high}} \quad _k(t); \tag{1.4}$$

where only two beamforming weight vectors $w_{\text{low}}$ and $w_{\text{high}}$ are exploited which, respectively, result in the sidelobe levels of $_{\text{low}}$ and $_{\text{high}}$ ( $_{\text{low}}$ < $_{\text{high}}$) at all the communication receivers. The value of each coefficient $b_k( )$ is either 0 or 1 during each radar pulse. These coefficients select the desired beamforming weight vector for each of the $K$ transmitted waveforms, thereby carrying one bit of information for each of these waveforms. During each radar pulse, a radar waveform is transmitted with an amplitude of either $_{\text{low}} \sqrt{P=K}$ or $_{\text{high}} \sqrt{P=K}$ towards each communication receiver

[1] see Section A.5 of Appendix A for detail.

for the detection of embedded information. This means that the same communication symbols are broadcast to all the receivers. Obviously, it is not possible to transmit di erent information streams to di erent communication users located at di erent directions.

Another ASK based JRC technique employs only one beamforming weight vector, which corresponds to the highest allowable sidelobe level at all the communication receivers resulting in highest possible SNR for the communication receivers. During each radar pulse, $\hat{K}$ 1 bits are transmitted such that the coe cients corresponding to $K$( $\hat{K}$ 1) bits are equal to 1 and the remaining $\hat{K}$ $K$ 1 bits are equal to 0. This is achieved by transmitting $\hat{K}$ distinct orthogonal waveforms. The transmitted signal is given as [23]:

$$s(t; \ ) = \sqrt{\frac{P}{K}} \sum_{k=1}^{\hat{K}\,X\,1} b_k(\ ) w_{high\ \ k}(t) + \sqrt{P} \sum_{k=1}^{\hat{K}\,Y\,1} (1 \quad b_k(\ )) \, w_{high\ \ \hat{K}}(t): \qquad (1.5)$$

Each coe cient $b_k(\ )$ for 1 $k$ $\hat{K}$ 1 is either 0 or 1 such that only $K$ coe cients are equal to 1 and the rest of them are equal to 0. The second term in the above equation expresses the case when all zeros are transmitted (i.e., all coe cients $b_k(\ )$ for 1 $k$ $\hat{K}$ 1 are equal to 0) using the reference orthogonal waveform $_{\hat{K}}(t)$. In this scheme, same information is broadcast to all the communication receivers because the transmission is formulated to achieve same sidelobe level at each communication receiver.

### 1.1.4 PSK Based Schemes

The fundamental principle underlying PSK based JRC is to embed communication information by controlling the phase of the signals transmitted towards the communication receivers while keeping the amplitude levels constant in the direction of communication [19, 24{26]. This is achieved by exploiting the radiation pattern in-

variance property of uniform linear arrays (ULAs) which states that, for each of the possible transmit radiation patterns, there exists a set of beamforming weight vectors $\mathbf{W}_r = [\mathbf{w}_1; \mathbf{w}_2; \ldots; \mathbf{w}_{2^{M-1}}]$ such that each column of $\mathbf{W}_r$ provides exactly the same radiation pattern but exhibits different phase profile. The complete set $\mathbf{W}_r$ can be determined if any of the beamforming vectors presented in $\mathbf{W}_r$ is known [46]. The transmitted signal for PSK based JRC can be expressed as [19, 24, 25]:

$$\mathbf{s}(t; \theta) = \sqrt{\frac{P}{K}} \sum_{k=1}^{K} \mathbf{W}_r \mathbf{b}_k(\theta) \phi_k(t); \quad K \geq \hat{K}; \tag{1.6}$$

where $\mathbf{b}_k(\theta)$ is a binary vector of size $(2^{M-1} \times 1)$ such that all of its elements are zero except one element which is equal to 1. The vector $\mathbf{b}_k(\theta)$ is responsible to select the desired beamforming vector $\mathbf{w}_k$ from $\mathbf{W}_r$. Here, $\mathbf{w}_1$ is calculated by solving the optimization problem in Eq. (1.2) and rest of the beamforming vectors in $\mathbf{W}_r$ are calculated using the method developed in [46]. If coherent communication is considered, each radar pulse consists of $K$ orthogonal waveforms transmitted towards communication receivers with the embedded phase information given as:

$$\phi_k = \angle \{ \mathbf{w}_k^H \mathbf{a}(\theta_r) \}; \quad 1 \leq k \leq K; \tag{1.7}$$

where $\angle\{\cdot\}$ denotes the angle of a complex number. For non-coherent communications, we select $\phi_1(t)$ as the reference waveform transmitted using the reference beamforming weight vector $\mathbf{w}_1$ by setting $\mathbf{b}_1(\theta) = [1; \mathbf{0}_{2^{M-1}-1}]^T$, where $(\cdot)^T$ is the transpose operator, and $\mathbf{0}_{2^{M-1}-1}$ is a row vector of all zeros having the length of $2^{M-1} - 1$. In this case, each radar pulse projects the set of $(K - 1)$ phase rotations towards the communication receivers. The phase $\phi_k$ corresponding to the $k$-th waveform can be calculated as:

$$\phi_k = \angle \left\{ \frac{\mathbf{w}_k^H \mathbf{a}(\theta_r)}{\mathbf{w}_1^H \mathbf{a}(\theta_r)} \right\}; \quad 2 \leq k \leq K. \tag{1.8}$$

## 1.2 Proposed Research Work

We primarily focus on spectrum sharing strategy based on JRC transmission, i.e. we consider the waveform transmission systems which satisfy the objectives of radar and communication systems simultaneously such that the same transmit waveforms are used by the both systems.

Important parts of our proposed research directions as follows:

### 1.2.1 Throughput Enhancement for Beamforming Based JRC Systems

We propose a novel JRC strategy to embed quadrature amplitude modulation (QAM) based communication information in the radar waveforms by exploiting sidelobe control and waveform diversity. The proposed information embedding technique can support multiple communication receivers located in the sidelobe region of the radar. In addition to the information broadcasting, the developed approach enables multi-user access by allowing simultaneous transmission of distinct information streams to the communication receivers located in di erent directions. We show that the proposed technique ensures a signi cant data rate enhancement compared to the existing techniques. Moreover, the developed JRC strategy generalizes the mathematical framework of the existing sidelobe control-based information embedding techniques. This research work is extensively discussed in Chapter 2.

### 1.2.2 Distributed JRC Systems

We present a novel distributed JRC MIMO system capable of simultaneously performing radar and communication tasks. The radar objective is to achieve the desired target localization performance whereas the communication objective is to optimize

the overall data rate. The distributed JRC MIMO system performs both objectives by optimizing the power allocation of the di erent transmitters in the JRC system. A dictionary of radar waveforms is used at each transmitter and the communication information is embedded in the radar waveform by exploiting waveform diversity. The proposed strategy can serve multiple communication receivers located in the vicinity of the distributed JRC MIMO system. We discuss this research work in Chapter 3.

### 1.2.3 Sensor Selection for Beamforming Based JRC Systems

Optimal sensor selection is anticipated as an attractive means to achieve superior performance with a low hardware cost because of the ever-decreasing cost of the sensor deployment compared to the radio frequency chains and processors. We will address optimal sensor selection for adaptive beamforming-based JRC systems by exploiting a constrained re-weighted $l_1$ norm minimization. Such minimization was originally proposed for the sparsity based regression problems. It has been observed that the re-weighted $l_1$ minimization approaches to $l_0$ norm minimization by solving an iterative convex problem. We are still progressing our research work in this direction and preliminary detail is included in Chapter 4.

In the following chapters, we will discuss these research directions in detail. Mathematical analysis and simulation results are provided to illustrate the performance of the proposed techniques.

## 1.3 Published Work

During his dissertation, the author has worked on three projects: (a) Spectrum sharing strategies for JRC systems, (b) spatial and temporal spectrum sensing, and (c) target parameter estimation for over-the-horizon radar. All the published work up till now is listed as follows:

1. A. Ahmed, Y. D. Zhang, and Y. Gu, \Dual-function radar-communications using QAM-based sidelobe modulation," Digital Signal Processing, vol. 82, pp. 166-174, Nov. 2018.

2. A. Ahmed, S. Zhang, and Y. D. Zhang, \Multi-target motion parameter estimation exploiting collaborative UAV network," IEEE International Conference on Acoustics, Speech, and Signal Processing, Brighton, U.K., May 2019.

3. A. Ahmed, Y. D. Zhang, and J-K. Zhang, \Coprime array design with minimum lag redundancy," IEEE International Conference on Acoustics, Speech, and Signal Processing, Brighton, U.K., May 2019.

4. A. Ahmed, Y. D. Zhang, and B. Himed, \Distributed dual-function radar-communication MIMO system with optimized resource allocation," IEEE Radar Conference, Boston, MA, April 2019.

5. A. Ahmed, Y. Gu, D. Silage, and Y. D. Zhang, \Power-e cient multi-user dual-function radar-communications," IEEE International Workshop on Signal Processing Advances in Wireless Communications, Kalamata, Greece, June 2018.

6. A. Ahmed, Y. D. Zhang, and B. Himed, \Multi-user dual-function radar-communications exploiting sidelobe control and waveform diversity," IEEE Radar Conference, Oklahoma City, OK, April 2018.

7. A. Ahmed, Y. D. Zhang, and B. Himed, \Cumulant-based direction-of-arrival estimation using multiple co-prime frequencies," Asilomar Conference on Signals, Systems, and Computers, Paci c Grove, CA, Oct. 2017.

8. A. Ahmed, Y. D. Zhang, and B. Himed, \E ective nested array design for fourth-order cumulant-based DOA estimation," IEEE Radar Conference, Seattle, WA, May 2017. (best student paper award { 3rd position)

# Chapter 2

# Throughput Enhancement of Beamforming Based Joint Radar-Communication Systems

In this chapter, we focus on the communication data rate enhancement of existing beamforming based JRC systems. We propose a novel quadrature amplitude modulation (QAM) based JRC strategy which exploits sidelobe control and waveform diversity, simultaneously, to transmit communication information. The proposed approach enables multi-user access such that we can send distinct QAM based communication streams in di erent directions while utilizing the same hardware resources as employed by the existing ASK and PSK based techniques. In this context, the proposed technique can provide a higher throughput compared to the conventional approaches, where multiplexing of communication information will be required to transmit di erent information to di erent receivers.

It is important to note that the author has developed an ASK based method [31] which enables multiple access contrary to the aforementioned ASK based methods. This objective is achieved by simultaneously transmitting di erent sidelobe levels

towards the communication receivers located in di erent directions. However, we omit the detail of that method because the following strategy discussed in this chapter is a generalized form and [31] can be considered a special case of this strategy.

In contrast to the prior multi-user ASK based scheme proposed by the author [31] which employs varying sidelobe levels at di erent communication receivers, the proposed strategy exploits varying sidelobe levels as well as phases of transmitted waveforms to further enhance the data rate. The data rate achieved by the proposed QAM based scheme is the sum of the data rate separately o ered by the amplitude and phase variations. Note that, unlike the existing PSK based schemes [19, 24, 25], which work only for ULAs to utilize the radiation pattern invariance property [46], the proposed approach also works for arbitrary arrays. Moreover, the proposed technique serves as the generalized mathematical model for the existing sidelobe ASK based JRC schemes. Simulation results demonstrate the e ectiveness of the proposed strategy.

The proposed QAM based sidelobe modulation scheme is di erent from the existing schemes in the following way:

The proposed approach enables multi-user access. Di erent communication users can be served with distinct communication streams, simultaneously. This is contrary to the existing JRC schemes which transmit the same communication information to all the users.

The proposed approach embeds the communication information as a QAM symbol containing the amplitude as well as the phase part. Existing schemes either use ASK or PSK based schemes which result in the reduced data rate for the same symbol space.

## 2.1 Proposed QAM Based Sidelobe Modulation

### 2.1.1 Signaling Strategy

We have observed that the existing ASK based JRC approaches [19{23] can only broadcast the same information to all the communication receivers by controlling the sidelobe levels during each radar pulse. Since the sidelobe levels towards all the communication directions are same, it is impossible to enable multi-user access, i.e., transmission of di erent information to the receivers located in di erent directions is not feasible. On the other hand, the PSK based JRC strategy can be enabled to transmit distinct communication streams to di erent users ; however, the use of radiation pattern invariance property [46] is restricted to ULAs only. Moreover, PSK based schemes cannot exploit the diversity achieved by the ASK principle, restricting the amount of data which can be transmitted. Nevertheless, it is possible to increase the maximum possible data rate by varying sidelobe levels for di erent communication receivers and exploiting an e cient PSK based JRC strategy. However, inability of ASK based schemes to transmit di erent communication streams in di erent directions makes the problem much more cumbersome.

In the proposed approach, a JRC system consisting of an arbitrary linear transmit antenna array can serve di erent communication receivers located in the sidelobe region with di erent communication information by exploiting QAM based communication, i.e., utilizing both amplitude and phase information simultaneously. The proposed JRC system is powered with two degrees-of-freedom (DOFs):

1. The information embedding exploits di erent amplitude levels to feed distinct communication streams to multiple communication users located in di erent directions. Such distinct information transmission is made possible by exploiting di erent sidelobe levels in di erent directions simultaneously during each radar

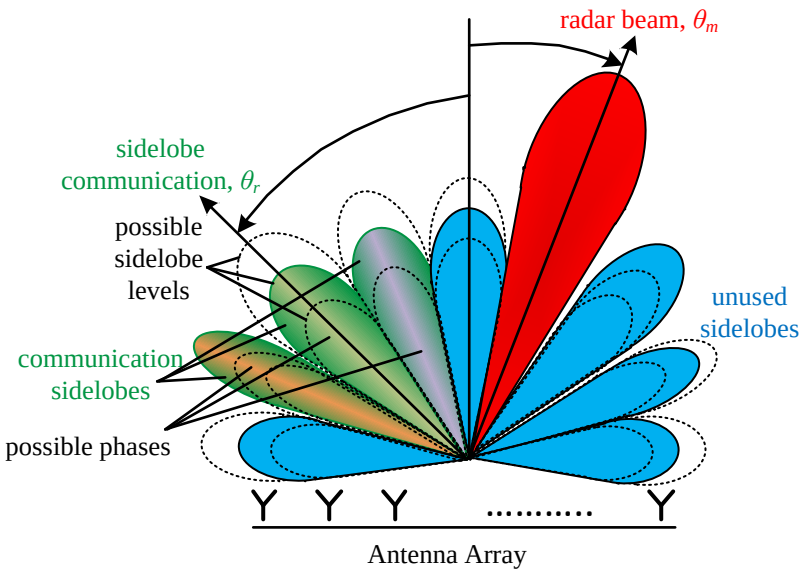


Figure 2.1: The proposed JRC strategy using QAM based sidelobe modulation.

pulse. These sidelobe levels are kept constant during each radar pulse which constitutes the symbol period.

2. The JRC system can transmit the symbols with di erent phase di erences in di erent directions, thus providing an extra DOFs in addition to the provision of multiple-level sidelobes.

The proposed scheme is analogous to QAM based communication system as it exploits amplitude as well as phase shift keying to enable the information embedding using multiple radar waveforms. Moreover, we will show that the proposed scheme serves as the generalized mathematical formulation of the existing JRC techniques [19{28]. Fig. 2.1 illustrates the basic principle of the proposed approach.

The beamforming weight vectors for the proposed QAM based communication scheme can be extracted by solving the following optimization:

$$\begin{aligned} &\min_{\mathbf{w}_n} \max_{m} \; e^{j\,'(\,m)} \quad \mathbf{w}_n^{\mathrm{H}}\mathbf{a}(\,_m) \;; \quad _m \; 2 \;; \\ &\text{subject to} \quad \mathbf{w}_n^{\mathrm{H}}\mathbf{a}(\,_p) \quad \text{''}; \quad _p \; 2 \;; \\ &\qquad\qquad \mathbf{w}_n^{\mathrm{H}}\mathbf{a}(\,_r) = \; _n(\,_r)e^{j\;_n(\,_r)}; \quad 1 \quad r \quad R; 1 \quad n \quad N: \end{aligned} \tag{2.1}$$

Here, $\mathbf{w}_n$ is the $n$-th beamforming weight vector resulting in sidelobe level $\ _n(\ _r)$ and phase $e^{j\ _n(\ _r)}$ towards the $r$-th communication receiver located at $\ _r$. Note that the sidelobe level $\ _n(:)$ and the projected phase $e^{j\ _n(\ _r)}$ are functions of angle $\ _r$ of the communication receivers. Each sidelobe level term $\ _n(\ _r)$ can take any of the $L$ allowable sidelobe levels and each phase term $e^{j\ _n(\ _r)}$ can take any of the $Q$ allowable phases. The beamforming weight vector $\mathbf{w}_n$ in Eq. (2.1) is constructed using $R$ communication constraints, each corresponding to the desired sidelobe level and phase towards the communication receiver located at di erent angles $\ _r$ ($1 \quad r \quad R$).

The possibility of having $L$ unique sidelobe levels and $Q$ unique phases results in $LQ$ unique combinations for the term $\ _n(\ _r)\ e^{j\ _n(\ _r)}$ towards $\ _r$. However, each of the $R$ communication constraints selects only one distinct value of $\ _n(\ _r)e^{j\ _n(\ _r)}$ out of the $LQ$ possible values for evaluating the beamforming weight vectors. Note that the values of $\ _n(\ _r)e^{j\ _n(\ _r)}$ can be di erent in di erent directions $\ _r$, thereby enabling multi-user access, i.e., ensuring independent communication streams towards di erent directions. Since there are $LQ$ possible values of $\ _n(\ _r)e^{j\ _n(\ _r)}$ at each communication receiver, there will be a total of $(LQ)^R$ possible communication constraints for the $R$ users. A beamforming weight vector $\mathbf{w}_n$ is designed by selecting $R$ constraints out of the total $(LQ)^R$ constraints. Therefore, we can generate $N = (LQ)^R$ unique beamforming weight vectors using Eq. (2.1) such that each beamforming weight vector projects a unique set of $R$ QAM symbols towards the communication directions. The desired beamforming weight vector corresponding to the required amplitude levels and phases towards communication directions can be selected from the set of $(LQ)^R$ beamforming weight vectors for information transmission.

For the proposed approach, it is possible to transmit radar waveforms with the same (broadcast case) or di erent (multi-user access case) information by respectively choosing the same or di erent sidelobe levels and phases at all the communication receivers simultaneously. The signal transmitted from the JRC antenna array is

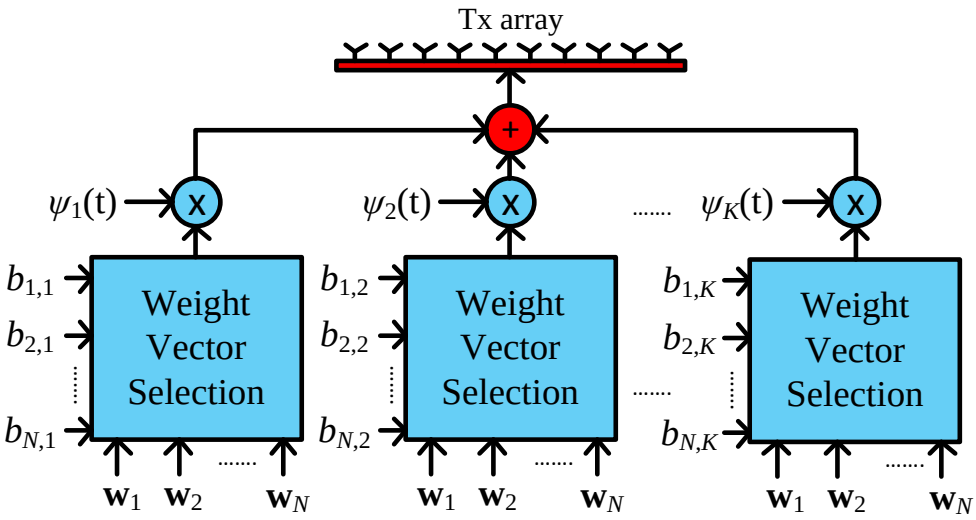


Figure 2.2: The proposed QAM based JRC approach using QAM based sidelobe modulation (coe cients $b_{n;k}$ are the function of ).

expressed as:

$$s(t; ) = \sqrt{\frac{P}{K}} \sum_{k=1}^{K} \mathbf{W}\, \mathbf{b}_k( )\ _k(t); \qquad (2.2)$$

where $\mathbf{W} = [\mathbf{w}_1; \mathbf{w}_2; \ldots; \mathbf{w}_N]$ is an $M$ $N$ matrix which serves as the dictionary of $N$ beamforming weight vectors optimized using Eq. (2.1), and $\mathbf{b}_k( ) = [b_{1;k}( ), b_{2;k}( ); \ldots; b_{N;k}( )]^T$ is an $N$ 1 binary selection vector selecting the desired beamforming weight vector from the dictionary $\mathbf{W}$ for each transmitted waveform $_k(t)$. Moreover, $t$ is the fast time and is the slow time index.[1] All the elements in $\mathbf{b}_k( )$ are 0 except only one element which is equal to 1. We utilize $K$ ( $\hat{K}$) orthogonal waveforms during each radar pulse and it is possible to use di erent values of $K$ for each pulse. Note that the individual sidelobe levels and phases towards each communication receiver obtained by the weight vectors present in $\mathbf{W}$ are not the same, thus enabling us to transmit distinct QAM based communication streams towards each communication receiver.

[1] see Section A.5 of Appendix A for detail.

The proposed transmission scheme allows $L$ unique sidelobe levels and Q unique phases at each receiver, each transmitted waveform carries $\log_2(LQ)$ bits of distinct information for each receiver. The proposed signaling strategy is outlined in Fig. 2.2.

The transmitted signal $s(t;\ )$ in (10) can be rewritten in a compact form as:

$$s(t;\ ) = \sqrt{\frac{P}{K}}\mathbf{W}\mathbf{B}(\ )\quad (t); \tag{2.3}$$

where

$$\begin{aligned} \mathbf{B}(\ ) &= \quad b_1(\ );\ \ b_2(\ );\quad\quad ;\ \ b_K(\ )\quad ; \\ (t) &= \quad {}_1(t);\quad {}_2(t);\quad\quad ;\quad {}_K(t)\quad ^{\mathsf{T}}: \end{aligned} \tag{2.4}$$

The radar system transmits waveforms in the form of pulses. For this purpose, we de ne *coherent communication* as the protocol where the start time of pulses is always known at the communication receivers. On the other hand, communication receivers are blind about the pulse start time in *non-coherent communication.* For both protocols, we assume that all the radar waveforms are known at the communication receivers. Since the start time of the pulses are known for coherent communications, all the orthogonal waveforms can be used to transmit information. On the other hand, a reference waveform (pilot tone) is reserved in non-coherent communication to detect the start time of the pulses. This is achieved by the sliding window matched lter ing with the reference waveform.

For the case of coherent communications where carrier synchronization is not an issue, the transmitted information in the direction $_r$ can be expressed as:

$$G_{\mathsf{T}}(\ _r) = \mathbf{w}_n^{\mathsf{H}}\mathbf{a}(\ _r) = \quad _n(\ _r)e^{j\ _n(\ _r)};\quad 1\quad n\quad N; \tag{2.5}$$

where $\quad _n(\ _r)$ and $e^{j\ _n(\ _r)}$ vary with respect to $\ _r$.

For the case of non-coherent communications where it is difficult to achieve carrier synchronization, we can exploit a reference waveform $\phi_1(t)$ along with a reference beamforming vector $\mathbf{w}_1$ (collectively forming the reference pilot tone). In this way, the transmitted information in the direction $\theta_r$ can be expressed as:

$$G_T(\theta_r) = \frac{\mathbf{w}_n^H \mathbf{a}(\theta_r)}{\mathbf{w}_1^H \mathbf{a}(\theta_r)}; \quad 2 \quad n \quad N: \tag{2.6}$$

Note in Eqs. (2.5) and (2.6) that $\mathbf{w}_n$ varies with $\quad$ depending on the value of $\mathbf{b}_k(\ )$ in Eq. (2.2), and $G_T(\theta_r)$ provides an estimate of the transmitted QAM symbol, where $|G_T(\theta_r)|$ and $\angle G_T(\theta_r)$ respectively represent the amplitude and the phase components of the transmitted QAM symbols in the communication direction $\theta_r$.

### 2.1.2 Information Decoding at Communication Receivers

The signal received at the $r$-th communication receiver located in the sidelobe region at angle $\theta_r$ can be described as:

$$x_r(t;\ ) = \alpha_r(\ )\mathbf{a}^T(\theta_r)\mathbf{s}(t;\ ) + n(t); \tag{2.7}$$

where $\alpha_r(\ )$ is the complex-valued channel response which is considered constant during each radar pulse, and $n(t)$ is the zero-mean complex white Gaussian noise. Matched filtering the received signal $x_r(t;\ )$ in (2.7) to each of the $K$ possible waveforms at the $r$-th communication receiver yields the following scalar output:

$$\begin{aligned} y_{r;k}(\ ) &= \frac{1}{T}\int_{t=0}^{T} x_r(t;\ )\,\phi_k(t)\,dt \\ &= \begin{cases} \sqrt{\frac{P}{K}}\,\alpha_r(\ )\,\beta_n(\theta_r)e^{j\varphi_n(\theta_r)} + n_k(\ ); & \text{if } \phi_k(t) \text{ was transmitted,} \\ n_k(\ ); & \text{otherwise.} \end{cases} \end{aligned} \tag{2.8}$$

Here, $n_k(\ )$ is the zero-mean complex white Gaussian noise at the output of the matched filter. By analyzing $y_{r;k}(\ )$ at the $r$-th receiver using all radar waveforms $_k(t)$, $1 \quad k \quad \hat{K}$, it is possible to determine the transmitted sidelobe levels $_n(\ _r)$ and phases $e^{j\ _n(\ _r)}$ which decodes the embedded communication information.

For the case of coherent communication, the receiver at $_r$ determines the transmitted QAM signals during each radar pulse as:

$$G_{\mathrm{R}}(\ _r) = y_{r;k}(\ ): \tag{2.9}$$

For the case of non-coherent communication, $y_{r;1}(\ )$ is considered as the reference, and the receiver determines the transmitted QAM signals during each radar pulse as:

$$G_{\mathrm{R}}(\ _r) = \frac{y_{r;k}(\ )}{y_{r;1}(\ )}: \tag{2.10}$$

In Eqs. (2.9) and (2.10), $G_{\mathrm{R}}(\ _r)$ denotes the received QAM communication symbol having magnitude $jG_{\mathrm{R}}(\ _r)j$ and phase $\backslash fG_{\mathrm{R}}(\ _r)g$ at the receiver located at angle $_r$.

We can observe that the proposed multi-waveform sidelobe QAM based signaling strategy treats each of the existing JRC techniques discussed in [19{28, 31] as a special case. Table 2.1 shows the parameters which can be changed in Eq. (2.2) to yield these existing JRC signaling methods. This implies that the proposed signaling scheme represents a generalized mathematical framework of existing JRC schemes [19{28, 31].

The following proposition addresses the number of users which can be supported by the proposed JRC technique.

**Proposition 1:** For the JRC system consisting of an $M$-element ULA, the number of maximum possible supportable communication users located in unique directions is $M \quad 1$.

**Proof:** For the case of ULA, we can consider the beamforming weight vector in Eq. (2.1) as a polynomial of degree $M-1$ having a maximum of $M-1$ unique roots. If all these $M-1$ roots correspond to the equality constraints in Eq. (2.1), it may still be possible to solve for other constraints without losing any DOFs in ideal cases. However, some of the DOFs might be utilized to satisfy the inequality constraint and the minimization function in Eq. (2.1). Thus, the maximum possible number of supported communication users located in distinct directions for ULA is $M-1$.

### 2.1.3 Sum Data Rate Analysis

In this section, we evaluate the sum of the number of bits which can be transmitted during one radar pulse using the proposed QAM based JRC technique to the sidelobe communication receivers located at distinct angles. We consider $R$ receivers utilizing $L(\geq 1)$ sidelobe levels and $Q(\geq 1)$ phase constellations with $LQ > 1$ such that $K = \hat{K}$ fixed number of orthogonal waveforms are used during each radar pulse. The following proposition addresses the achievable data rate.

**Proposition 2:** The maximum data rate achieved from the proposed QAM based JRC strategy is $RK\log_2(LQ)$ for coherent communication.

**Proof:** According to Eq. (2.2), for each radar waveform $\psi_k(t)$, we can transmit $L$ possible sidelobe levels and $Q$ distinct phases to each communication receiver. Thus, each communication receiver deciphers $\log_2(LQ)$ bits of distinct information during each radar pulse for each of the $K$ transmitted radar waveforms. Therefore, the sum data rate for all the $R$ communication receivers becomes $RK\log_2(LQ)$ for the case of coherent communications. Similarly, the sum data rate offered by the proposed strategy for non-coherent communication is $R(K-1)\log_2(LQ)$ if one waveform is used as the reference waveform.

Table 2.1: Generalization of the existing beamforming JRC based strategies by the proposed technique

| Signaling Strategy | Parameters for Eq. (2.1)-(2.2) | Maximum data rate (bits/pulse) |
|---|---|---|
| Sidelobe AM [20] | $K = 1; N = L \quad 2;$ $Q = 1; R = 1.$ | $\log_2 L$ |
| Multiwaveform ASK [21, 22] | $N = L = 2; Q = 1;$ xed $K$ ( $\hat{K}$ ); varying $R;$ $u_1 = u_{low}; u_2 = u_{high};$ $b_{1;k}(\ ) = 1 \quad b_{2;k}(\ )$ | $K \log_2 L$ |
| Multi-waveform single-level ASK[23] | $N = L = 1; Q = 1;$ $u_1 = u_{high};$ varying $K$ and $R,$ For all zeros: $K = 1; b_{1;K} = 1$ else: $b_{1;1} = 0;\ b_{1;k} = 0$ or 1, $\sum_{k=2} b_{1;k} = K.$ | $K \quad \hat{K}$ |
| Multi-user ASK [31] | varying $N; L; R; K;$ $Q = 1;\ 1 < K \quad \hat{K}$ | $RK \log_2 L$ |
| Multi-waveform coherent PSK [25, 26] | $N = L = 1; u_1 = u_{high};$ xed $K$ ( $\hat{K}$ ), varying $R$ and $Q$( 2). | $K \log_2 Q$ |
| Multi-waveform non-coherent PSK [25, 26] | $N = L = 1; u_1 = u_{high};$ xed $K(2 \quad K \quad \hat{K})$, varying $R$ and $Q$( 2) | $(K \quad 1) \log_2 Q$ |
| Coherent Multi-user QAM (proposed) | varying $N; L; R; Q; K$ | $RK \log_2 LQ$ |
| Non-coherent Multi-user QAM (proposed) | varying $N; L; R; Q; K;$ $1 < K \quad \hat{K}$ | $R(K \quad 1) \log_2 LQ$ |

The achievable data rate o ered by the proposed QAM based information embedding strategy is compared with existing JRC methods [19{28, 31] in Table 2.1. It is evident that the proposed technique outperforms existing approaches in terms of overall throughput or sum data rate because it bene ts from multiple sidelobe levels and

phase possibilities simultaneously at di erent communication receivers. Moreover, the ability to transmit di erent information streams (sidelobe levels and phases) to di erent users further enhances the maximum achievable data rate.

## 2.2 Simulation Results

In this section, we present simulation results to illustrate the performance of the proposed QAM based JRC strategy. In all simulations, we consider a ULA of 10 transmit antennas to serve two communication users located in the sidelobe region of the radar. We have used CVX toolbox [47{50] with MATLAB to solve all the optimizations. Moreover, communication system protocol is also modeled in MATLAB.

### 2.2.1 Beampattern Synthesis and Data Rate Analysis for Equal Number of Sidelobe Levels and Phase Constellations

We consider that the JRC system is capable of projecting two sidelobe levels and can transmit the waveforms with two di erent phases towards the communication receivers located in the sidelobe region at angles $35^o$ and $45^o$, respectively. For this case, we have $R = L = Q = 2$. Here, the primary function of the radar is to project the main beam at $0^o$. For the communication purpose, ASK and PSK based schemes will have the ability to exploit only the magnitude or phase variation, respectively. In contrast, the QAM based scheme can utilize the variation in both magnitude as well as the phase of the transmitted waveform.

Fig. 2.3(a) shows the transmit power pattern corresponding to two beamforming weight vectors for multi-waveform ASK [21, 22]. These beamforming vectors respectively broadcast the amplitude of either 30 dB or 40 dB in the directions

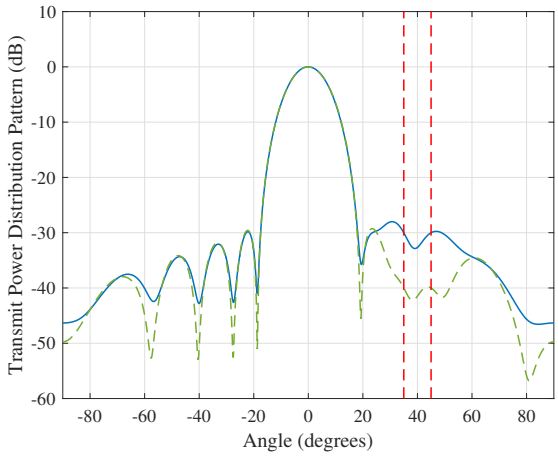


(a)

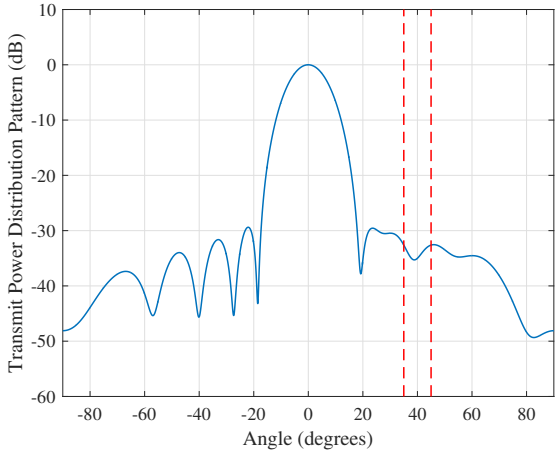


(b)

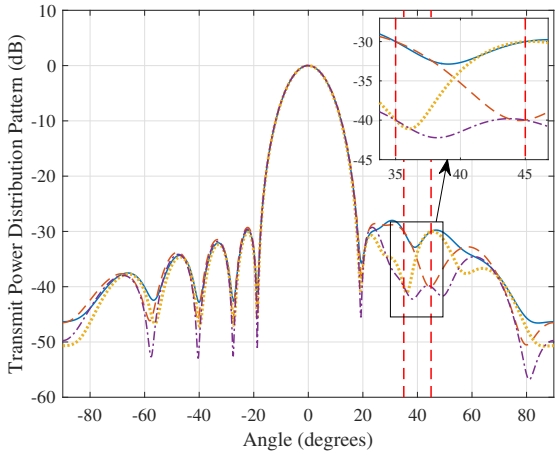


(c)

Figure 2.3: Beampatterns for JRC strategies ($R = 2; Q = 2; L = 2$): (a) Multi-waveform ASK based method [21, 22], (b) Multi-waveform PSK based method [24{ 26], (c) Proposed QAM based method.

of communication receivers. The sidelobe level at both communication receivers also remains identical for the existing ASK based schemes [21, 22] during each radar pulse. For PSK based method [24{26], two beamforming vectors are generated to have the same magnitude response but di erent phase response in the directions of communication receivers. Fig.2.3(b) shows the power pattern of these beamforming weight vectors projecting a sidelobe level of 32:61 dB at both communication receivers. Each of the two beamforming vectors for the PSK based method broadcast a unique phase towards all the communication receivers during each radar pulse. Just like ASK based methods, the transmitted information is broadcast to all the communication users.

Unlike the ASK based technique, the QAM based method can assign di erent sidelobe levels at the two communication receivers. Moreover, in contrast to the existing PSK based strategy, the proposed QAM based technique can transmit di erent phases to di erent receivers at the same time. Thus, the QAM based strategy can independently project two di erent levels of amplitudes as well as phases at the two receivers so as to transmit distinct information to each user. We can generate 16 beamforming weight vectors for $R = 2; L = 2; Q = 2$ using Eq. (2.1). Fig. 2.3(c) shows the four possible power patterns for the proposed QAM based scheme generated using Eq. (2.1). Since the number of possible transmitted phases towards each receiver are 2, each beampattern for the QAM based scheme corresponds to four distinct beamforming weight vectors projecting the same magnitude but di erent phase responses towards the two communication receivers.

Let us examine the achievable throughput (sum data rate) for this experiment. Note that the average power transmitted to each communication receiver is kept constant for all the three schemes. For a single radar waveform, the ASK based method exploiting two sidelobe levels will be able to transmit (broadcast) $\log_2 L = 1$ bit per waveform for each radar pulse. Coherent PSK based method utilizing two

phase options will also be able to broadcast $\log_2 Q = 1$ bit per radar waveform for each radar pulse. On the other hand, the coherent QAM based information embedding strategy is able to transmit 2 bits per user resulting in a total throughput of $R \log_2(LQ) = 4$ bits transmitted using each radar waveform during each radar pulse. For two waveforms, this data rate for all the coherent schemes will double. The non-coherent schemes will utilize one waveform as the reference and one waveform will be used for communication purpose; therefore, the data rate of coherent scheme will be half compared to the coherent counterpart if two orthogonal waveforms are utilized. Fig. 2.5 shows the maximum throughput with respect to the number of available waveforms for this simulation parameters ($R = L = Q = 2$). The simulation results clearly illustrate the superiority of our proposed technique in terms of sum data rate.

### 2.2.2 Bit Error Rate Analysis for Same Overall Throughput

In the second example, we investigate the possibility of synthesizing beamforming weight vectors for the case of extended radar's main beam and compare the bit error rate (BER) for the JRC strategies by keeping the sum data rate and transmitted power constant.

We consider two communication users ($R = 2$) at $35^o$ and $42^o$ with respect to the JRC transmit antenna array. The desired main lobe region is from $-10^o$ to $10^o$ and two orthogonal waveforms ($K = 2$) are available to the JRC system. The objective is to transmit 4 bits of information to each communication user (a total throughput of 8 bits).

For the case of multi-waveform ASK [21, 22], we have to design 16 beamforming weight vectors having sidelobe levels uniformly distributed from 0 to 0:1 towards the intended communication directions ($L = 16$; $K \log_2 L = 8$ bits throughput). For the PSK based technique [25, 26], 16 beamforming vectors having sidelobe level of 0:2347 towards the communication users are synthesized such that the respective phases of

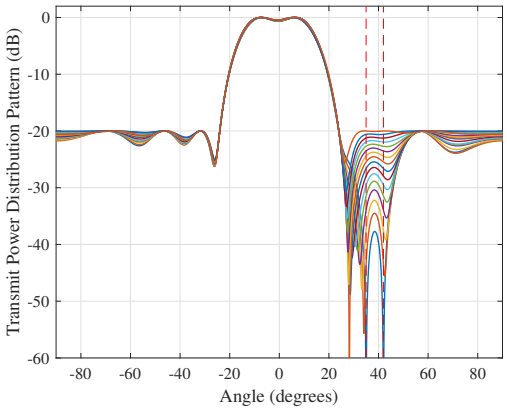


(a)

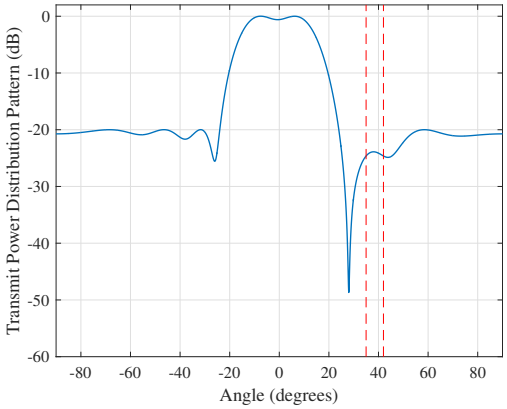


(b)

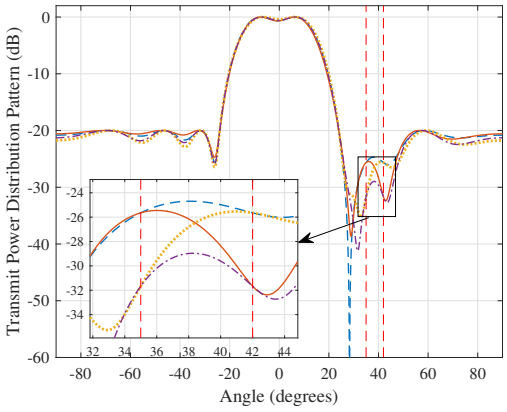


(c)

Figure 2.4: Beampatterns for JRC strategies. (a) Multi-waveform ASK based method [21, 22], (b) Multi-waveform PSK based method [24{26], (c) Proposed QAM based method

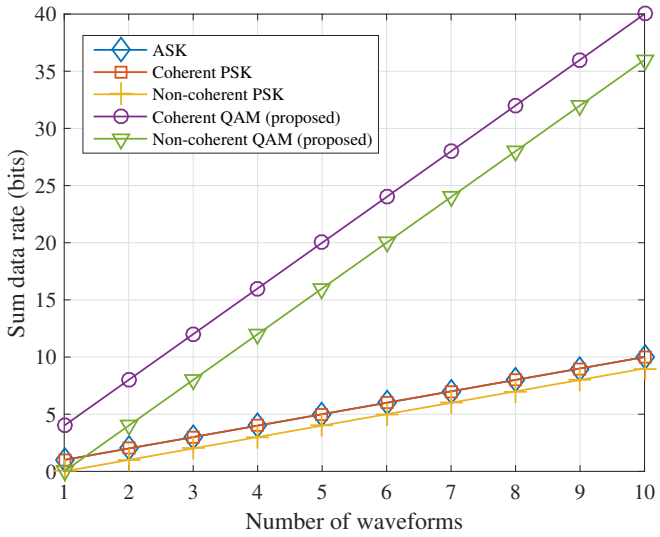


Figure 2.5: The comparison of throughput for the case of $R = L = Q = 2$ and varying number of available waveforms.

these beamforming vectors at the receivers is uniformly distributed from $0^o$ to $360^o$ ($Q = 16$; $K \log_2 Q = 8$ bits throughput).

Since there are only two available waveforms, the non-coherent PSK will have 32 beamforming weight vectors to match the data rate because one waveform will be used as a reference to realize non-coherent communications ($Q = 32$; $(K \quad 1) \log_2 Q = 8$).

For the case of the proposed coherent QAM based sidelobe modulation, we have generated 16 beamforming vectors using Eq. (2.1) such that there are a total number of four groups of QAM based beamforming weight vectors corresponding to the same amplitude response. Each group comprises four beamforming weight vectors corresponding to unique phase combinations at the both communication receivers. We have the ability to transmit waveforms towards the communication receivers with two distinct power levels and four phase possibilities. In a similar manner, the non-coherent QAM based strategy will result in the generation of 32 beampatterns such that we have the ability to project the radar waveforms at two power levels and four unique phase constellations at each communication receiver.

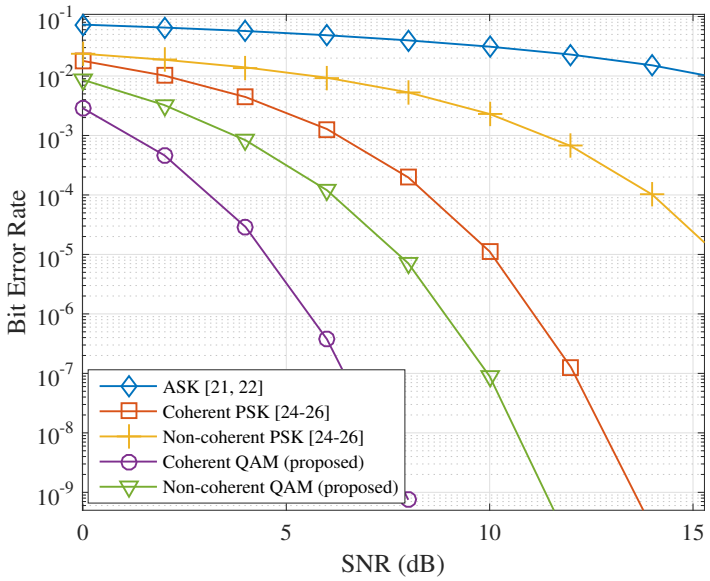


Figure 2.6: Bit error rate analysis for the multi-waveform ASK based method [21, 22], multi-waveform PSK based method (coherent and non-coherent case) [24{26] and the proposed QAM based method (coherent and non-coherent case).

The beampatterns for the designed beamforming vectors for the case of ASK, PSK and QAM based information embedding is shown in Fig. 2.4. We observe that the multi-waveform ASK and all the coherent communication based algorithms result in an equal number of beamforming weight vectors. Moreover, non-coherent based JRC techniques also have the same number of beamforming vectors.

Fig. 2.6 compares the BER performance of the proposed technique with existing techniques. For error reduction, all the symbols for the JRC transmission schemes are grey coded before transmission. We observe that the proposed QAM based method is more capable to resilient to noise compared to existing JRC techniques. This is because the proposed QAM based method is designed to o er a higher throughput with the same resources and, therefore, results in increased distance between the signals in the symbol space. The QAM symbol space in this simulation contains 8 symbols compared to 16 symbols each for PSK and ASK, respectively. In addition to this, 8-QAM symbols are distributed as two levels of amplitudes and 4 levels of phases which further increases the e ective distance between the transmitted symbol

constellations. This increased distance between the symbol constellations along with the exibility to transmit di erent symbols to di erent users results in reduced BER for the proposed QAM based technique. Moreover, the coherent communication based methods have better performance compared to the non-coherent counterparts because the number of symbols in the symbol space is increased for the latter, resulting in higher error rates. However, the proposed non-coherent QAM based information embedding strategy still outperforms the existing methods in terms of the BER.

In short, the simulation results illustrate the e ectiveness of the proposed QAM based information embedding in comparison to the existing schemes in terms of BER and the overall throughput of the communication system.

## 2.3 Remarks

A novel multi-waveform QAM based scheme exploiting sidelobe control and waveform diversity was proposed, which enables the transmission of distinct communication information to the communication receivers located in distinct directions. The information embedding has been discussed for coherent as well as non-coherent communication cases. Compared to the existing ASK and PSK based signaling strategies, the proposed method achieves higher transmission capacity by simultaneously enabling both amplitude and phase shift keying in the radar sidelobe region. Moreover, the ability to transmit distinct information in di erent directions enhances the sum data rate by a factor of number of communication users. As such, the proposed signaling strategy also serves as a generalized mathematical framework of existing JRC strategies. Simulation results evidently verify the e ectiveness of the proposed scheme.

# Chapter 3

# Distributed Joint Radar-Communication System

In this chapter, we propose a novel distributed JRC multiple-input multiple-output (MIMO) system capable of simultaneously performing radar and communication tasks. Note that this is the first research effort in this direction where spectrum sharing in a distributed radar-communication network is considered.

The radar objective is to achieve the desired target localization performance whereas the communication objective is to optimize the overall data rate. The distributed JRC MIMO system performs both objectives by optimizing the power allocation of the different transmitters in the JRC system. A dictionary of radar waveforms is used at each transmitter and the communication information is embedded in the radar waveform by exploiting waveform diversity. The proposed strategy can serve multiple communication receivers located in the vicinity of the distributed JRC MIMO system. Simulation results illustrate the performance of the proposed strategy.

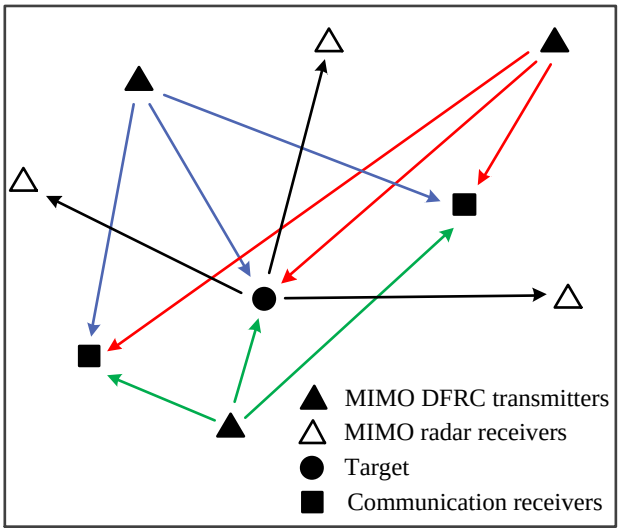


Figure 3.1: Distributed DRFC MIMO system.

## 3.1 System Model

### 3.1.1 Radar Subsystem

Consider a narrowband distributed MIMO radar system consisting of $M$ transmitters and $N$ receivers, which are arbitrarily located in a two-dimensional (2-D) coordinate system at the locations $(x_m; y_m)$ and $(x_n; y_n)$, respectively, for $1 \quad m \quad M$ and $1 \quad n \quad N$. Assume a point target located at $(x; y)$. The radar acts as a distributed JRC MIMO system whose primary objective is to track the target location. A coarse estimate of the parameters related to the target's radar cross-section (RCS)[1] and position is assumed available from the previous cycles. During each radar pulse, each transmitter radiates a unit-power orthogonal waveform $s_m(t)$, such that $(1=T) \int_0^T j s_m(t) j^2 dt = 1$ and $(1=T) \int_0^T s_m(t) s_n(t) dt = 0$ for $m \neq n$, where $T$ is the duration of each pulse and $t$ is the fast time.[2] Fig. 3.1 illustrates the JRC MIMO system.

[1] see Section A.2.1 of Appendix A for detail.
[2] see Section A.5 of Appendix A for detail.

The radar signal corresponding to the $m$-th transmitter and the $n$-th receiver is expressed as:

$$s_{m;n}(t) = \sqrt{p_{m;n} p_{m_{\text{tx}}}}\, h_{m;n} s_m(t - \tau_{m;n}) + w_{m;n}(t); \tag{3.1}$$

where $\alpha_{m;n}$ represents the signal variation due to path loss effects, $p_{m_{\text{tx}}}$ is the transmit power of signal $s_m(t)$ emitted from the $m$-th transmitter, $h_{m;n}$ denotes the target RCS[3] for the propagation path from the $m$-th transmitter to the $n$-th receiver, and $w_{m;n}(t) \sim CN(0; \sigma_w^2)$ represents the circularly symmetric zero-mean complex white Gaussian noise. The propagation delay $\tau_{m;n}$ due to the propagation path from the $m$-th transmitter to the $n$-th receiver is denoted as $\tau_{m;n} = (D_{m\text{tx}} + D_{n\text{rx}})/c$; where $D_{m\text{tx}}$ and $D_{n\text{rx}}$ are the range to target from the $m$-th transmitter and that from the $n$-th receiver, respectively, and $c$ is the propagation velocity of the transmitted signals. The path loss factor takes the form of $\alpha_{m;n} \propto 1/D_{m_{\text{tx}}}^2 D_{n_{\text{rx}}}^2$. Moreover, let $\mathbf{h} = [h_{1;1}; h_{1;2}; \ldots; h_{M;1}; h_{2;1}; \ldots; h_{M;N}]^{\text{T}}$ be the $MN \times 1$ vector of all bi-static RCS of the targets, and $\mathbf{p}_{\text{tx}} = [p_{1_{\text{tx}}}; p_{2_{\text{tx}}}; \ldots; p_{M_{\text{tx}}}]^{\text{T}}$ be the $M \times 1$ vector containing all the transmit powers from all transmitters of the JRC system.

We will optimize the total transmit power for the desired localization error performance for the radar subsystem. Lets denote $\mathbf{p}_{\text{tx;max}} = [p_{1_{\text{tx;max}}}; p_{2_{\text{tx;max}}}; \ldots; p_{M_{\text{tx;max}}}]^{\text{T}}$ and $\mathbf{p}_{\text{tx;min}} = [p_{1_{\text{tx;min}}}; p_{2_{\text{tx;min}}}; \ldots; p_{M_{\text{tx;min}}}]^{\text{T}}$ be the $M \times 1$ vectors respectively representing the maximum and the minimum allowable transmit power from the $M$ transmitters. We further denote $P_{\text{total}_{\text{max}}} \triangleq \sum_{m=1}^{M} p_{m_{\text{tx;max}}}$ as the maximum allowable power to be transmitted from the JRC transmitters collectively.

The Cramer-Rao Bound (CRB) expresses a lower bound on the variance of unbiased estimators of a deterministic (fixed, though unknown) parameter and serves as a popular performance metric. Here, the radar performance is evaluated in terms of the CRB representing the lower bound on the mean squared error of the target's

[3] see Section A.5 of Appendix A

location estimates. For the case of distributed radar, CRB is derived in [51{53] as:

$$_{x;y}(\mathbf{p}_{tx}) = \frac{\mathbf{q}^T \mathbf{p}_{tx}}{\mathbf{p}_{tx}^T \mathbf{A} \mathbf{p}_{tx}}; \tag{3.2}$$

where $\mathbf{q} = \mathbf{q}_a + \mathbf{q}_b$, $\mathbf{A} = \mathbf{q}_a \mathbf{q}_b^T \quad \mathbf{q}_c \mathbf{q}_c^T$, $\mathbf{q}_a = [q_{a_1}; q_{a_2}; : : : ; q_{a_M}]^T$, $\mathbf{q}_b = [q_{b_1}; q_{b_2}; : : : ; q_{b_M}]^T$ and $\mathbf{q}_c = [q_{c_1}; q_{c_2}; : : : ; q_{c_M}]^T$. Here,

$$\begin{aligned}
q_{a_m} &= \sum_{n=1}^{N} {}_{m;n} |h_{m;n}|^2 \left( \frac{x_m - x}{D_{m_{tx}}} + \frac{x_n - x}{D_{n_{rx}}} \right)^2; \\
q_{b_m} &= \sum_{n=1}^{N} {}_{m;n} |h_{m;n}|^2 \left( \frac{y_m - x}{D_{m_{tx}}} + \frac{y_n - x}{D_{n_{rx}}} \right)^2; \\
q_{c_m} &= \sum_{n=1}^{N} {}_{m;n} |h_{m;n}|^2 \left( \frac{x_m - x}{D_{m_{tx}}} + \frac{x_n - x}{D_{n_{rx}}} \right) \left( \frac{y_m - x}{D_{m_{tx}}} + \frac{y_n - x}{D_{n_{rx}}} \right);
\end{aligned} \tag{3.3}$$

where $_m = 8 \ ^2 B_m^2 / (\ _w^2 c^2)$, and $B_m$ is the e ective bandwidth of the signal transmitted from the $m$-th transmitter.

### 3.1.2 Communication Subsystem

Consider $R$ communication receivers that are located in the vicinity of the distributed JRC MIMO system. Assume that the signals re ected from the radar target and received at each communication receiver have a signi cantly lower magnitude compared to the line-of-sight transmission from the transmitters and, thus, are ignored. Then, we can express the received signal at the $r$-th ($1 \quad r \quad R$) receiver as:

$$s_{m;r}(t) = \sqrt{{}_{m;r} p_{m_{tx}}} g_{m;r} s_m(t \quad {}_{m;r}) + w_{m;r}(t); \tag{3.4}$$

where $g_{m;r}$ denotes the complex channel gain, $_{m;r}$ is the propagation delay, and $_{m;r} \ / \ D_{m;r}^2$ incorporates the path loss e ects, and $D_{m;r}$ is the distance between the $m$-th transmitter and the $r$-th communication receiver. We assume $w_{m;r}(t)$ $CN(0; \ _{m;r})$ be circularly complex white Gaussian noise whose statistics are known at the transmitter. The channel state information, expressed as the complex channel

gain vector $\mathbf{g} = [g_{1;1}; g_{1;2}; \ldots; g_{M;1}; \ldots; g_{M;R}]^{\mathrm{T}}$, is also assumed to be known at the radar fusion center.

The communication performance is evaluated in terms of the achieved Shannon capacity. The data rate from the $m$-th transmitter to the $r$-th receiver is expressed in terms of Shannon's capacity as:

$$<_{m;r} = \log_2 \left(1 + \frac{|g_{m;r}|^2 p_{m_{\mathrm{tx}}}}{\Gamma_{m;r}\, \sigma^2_{m;r}}\right) = \log_2 \left(1 + \frac{p_{m;\mathrm{tx}}}{\Gamma_{m;r}}\right); \tag{3.5}$$

where $\Gamma_{m;r} \geq 1$ represents the signal-to-noise ratio (SNR) gap which translates the loss in the data rate into the loss in the SNR and is determined by the coding scheme, and $\Gamma_{m;r} = \Gamma_{m;r}\, \sigma^2_{m;r}/|g_{m;r}|^2$. The sum data rate per radar pulse can be calculated as $< = \sum_{m=1}^{M} \sum_{r=1}^{R} <_{m;r}$.

# 3.2 Optimal Power Allocation for Distributed JRC MIMO System

## 3.2.1 Radar-Only Operation

The optimal power allocation for radar-only operation is derived in [52] as:

$$\begin{aligned} &\text{minimize} && 1_{1 \times M}\, \mathbf{p}_{\mathrm{tx}} \\ &\text{subject to} && \mathbf{p}_{\mathrm{tx;min}} \leq \mathbf{p}_{\mathrm{tx}} \leq \mathbf{p}_{\mathrm{tx;max}}; \\ & && \Gamma_{x;y}(\mathbf{p}_{\mathrm{tx}}) = \ldots \end{aligned} \tag{3.6}$$

The optimization in (3.6) minimizes the total transmit power for the distributed MIMO radar such that a desirable localization accuracy, described in terms of the CRB , is achieved. The optimization problem (3.6) can be relaxed to the following

convex form [52]:

$$\begin{aligned} \text{minimize} \quad & 1_{1 \times M} p_{tx} \\ \text{subject to} \quad & p_{tx;min} \leq p_{tx} \leq p_{tx;max}; \\ & q - A p_{tx} \leq 0: \end{aligned} \tag{3.7}$$

The solution of the convex optimization problem (3.7) yields the optimized transmit power vector $p_{tx;opt}$; which can be used as a starting point for a local optimization applied to the original optimization (3.6).

### 3.2.2 Communication-Only Operation

We assume that the waveform transmitted from each transmitter is broadcast to all communication users located in the vicinity of the JRC transmitters. We also assume that the channel side information is known at the JRC transmitter and communication receivers. We optimize the power allocation for communication operation by exploiting the conventional water- lling approach [54]. In such an approach, the transmit power is ampli ed for each user to the pre-determined power level compensating for the channel impairments. The desired power level is determined by considering the signal-to-noise (SNR) ratio of each user with the JRC transmitters. Generally, water- lling approach invests more resources in the communication channels which have better SNR.

The water- lling for the maximum allowable transmit power is achieved by solving the following equation simultaneously for all the communication receivers ($1 \leq r \leq R$):

$$\begin{bmatrix} p_{tx} \\ X_r \end{bmatrix} = \begin{bmatrix} P_{total_{max}} \\ r \end{bmatrix}; \tag{3.8}$$

where

$$U = \begin{bmatrix} 1_{1\times M} & 0 \\ I_{M\times M} & -1_{1\times M}^{T} \end{bmatrix}; \qquad {}_{r} = \begin{bmatrix} {}_{1;r} \\ {}_{2;r} \\ \vdots \\ {}_{M;r} \end{bmatrix};$$

where $X_r$ represents the water- lling power level. Eq. (3.8) may provide di erent optimal power distributions for di erent communication users depending on their channel side information. Moreover, the solution of Eq. (3.8) can also provide negative power if any channel has a deep fade. Therefore, we can write Eq. (3.8) for all the communication receivers as the following constrained least-square optimization problem:

$$\begin{aligned} \text{minimize} \quad & \sum_{r=1}^{R} X_r \left\| V \begin{bmatrix} p_{tx} \\ X_r \end{bmatrix} - {}_{r} \right\|_2^2 \\ \text{subject to} \quad & p_{tx;min} \quad p_{tx} \quad p_{tx;max}; \\ & 1^{T} p_{tx} \quad P_{total_{max}}; \\ & X_r \quad 0; \quad r = 1;2;:::;R; \end{aligned} \tag{3.9}$$

where $V = \begin{bmatrix} I_{M\times M} & -1_{1\times M}^{T} \end{bmatrix}$ and $\| \|_2$ is the $l_2$ norm. Note that $X_r$ is a free parameter and its optimal value is also determined by the above optimization. The optimization problem (3.9) is convex. However, unlike (3.6) and (3.7) where the least power required for satisfactory radar operation is extracted, it utilizes the maximum allowable power and distributes it with respect to channel quality for all the communication users. For a given maximum power $P_{total_{max}}$, the optimization problem (3.9) tends to maximize the water- lling level $X_r$, thus resulting in high data rate for the communication channels which have better channel conditions.

### 3.2.3 Joint Radar-Communication System

The optimal power allocation extracted from the optimization problems (3.7) and (3.9), respectively designed for radar-only and communication-only operations, are not favorable for the acceptable joint operation JRC system. The power allocation from optimization (3.7) provides the minimal required power from all the transmitters of the distributed radar. As such, this scheme may not establish an acceptable communication data rate as most of the transmitters work on a low power in ideal radar conditions, resulting in unacceptable SNR and data rate for communication users. Moreover, the resulting power from the optimization problem (3.7) is independent of the communication channel side information. Likewise, the resource allocation from the optimization problem (3.9) is not suitable for radar operation as the power distribution for this case is independent of the radar performance and may result in unacceptable target tracking performance, even after the maximum allowable power is utilized.

We can add the radar performance constraint in the optimization problem (3.9) to obtain the following modified convex optimization problem:

$$
\begin{aligned}
\text{minimize} \quad & \sum_{r=1}^{R} \left\| \begin{bmatrix} \mathbf{p}_{tx} \\ \mathbf{p}_{tx} \end{bmatrix} \right\|_{X_r}^{2} \\
\text{subject to} \quad & \mathbf{p}_{tx;min} \leq \mathbf{p}_{tx} \leq \mathbf{p}_{tx;max}; \\
& \mathbf{q} \leq \mathbf{A}\mathbf{p}_{tx} \leq 0; \\
& \mathbf{1}^{T}\mathbf{p}_{tx} \leq P_{total_{max}}; \\
& X_r \succeq 0; \quad r = 1; 2; \ldots; R.
\end{aligned}
\tag{3.10}
$$

The optimization problem (3.10) provides the optimal power allocation for distributed JRC transmitters under the maximum allowable power constraint such that the localization error for the radar operation is bounded by . At the same time, our objective

function tends to maximize the water- lling level $X_r$ to improve the communication data rate.

## 3.3 Information Embedding

The information embedding can be accomplished by utilizing waveform diversity. If each transmitter is assigned a dictionary of $K$ radar waveforms, the total bits transmitted from the distributed JRC MIMO system during one radar pulse is $M \log_2 K$, provided that the dictionaries are non-overlapping and all transmitters are active.

The signal received at the communication receiver $r$ can be expressed as:

$$\begin{aligned} s_r(t) &= \sum_{m=1}^{M} s_{m;r}(t) \\ &= \sum_{m=1}^{M} \sqrt{p_{m;r} p_{m_{tx}}}\, g_{m;r}\, s_m(t - \tau_{m;r}) + w_r(t); \end{aligned} \tag{3.11}$$

where $w_r(t) = \sum_{m=1}^{M} w_{m;r}(t)$. Matched $\lter$ing can be exploited at the communication receivers to synthesize the embedded information by feeding the time delayed versions of $s_r(t)$ in the matched $\lter$ as follows:

$$\begin{aligned} y_r(k) &= \frac{1}{T} \int_0^T s_r(t + k\,\Delta t) s_m(t)\, dt \\ &= \begin{cases} \sqrt{p_{m;r} p_{m_{tx}}}\, g_{m;r} + w_{r;k}(t); & \text{if } s_m(t) \text{ transmitted,} \\ w_{r;k}(t); & \text{otherwise;} \end{cases} \end{aligned} \tag{3.12}$$

where $\Delta t$ is the time delay de ning the time resolution of delay matched $\lter$ing, $k$ is a non-negative integer with $0 \le k \le T/\Delta t$ and $w_{r;k}(t)$ is the noise output.

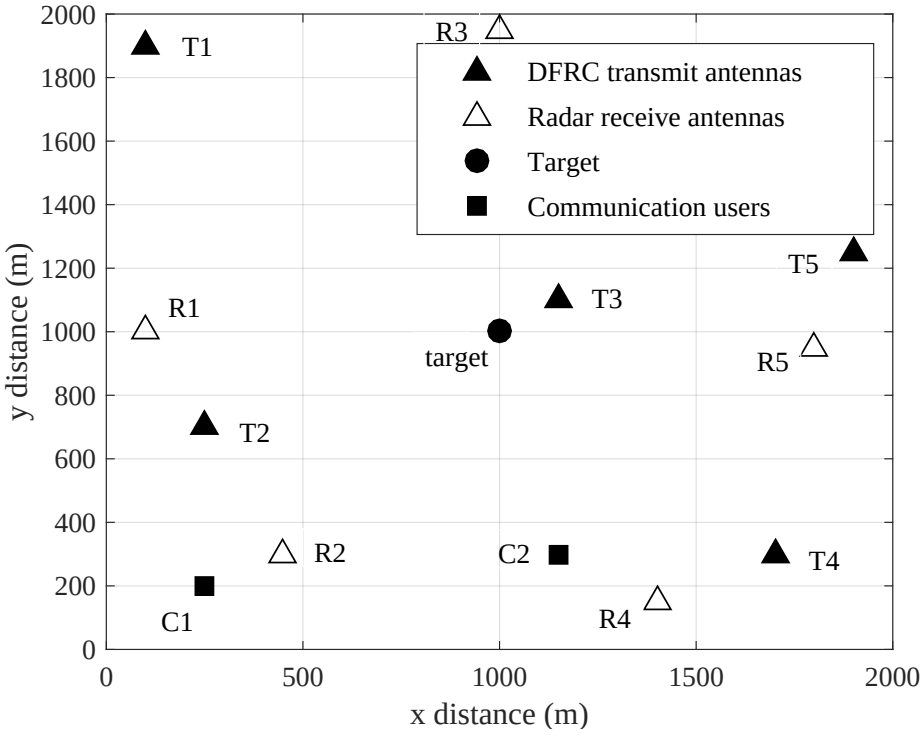


Figure 3.2: Simulation layout for distributed JRC MIMO system.

## 3.4 Simulation Results

Consider a distributed JRC MIMO system consisting of $M = 5$ isotropic transmitters located at (100; 1900) m, (250; 700) m, (1150; 1100) m, (1700; 300) m and (1900; 1250) m, respectively, in the two-dimensional space. The radar uses $N = 5$ receive antennas located at (100; 1000) m, (450; 300) m, (1000; 1950) m, (1400; 150) m and (1800; 950) m, respectively. A point target is located at the coordinate of (1000; 1000) m. Two communication receivers are located at (250; 200) m and (1150; 300) m, respectively. Fig. 3.2 shows the arrangement of the distributed JRC MIMO system and the communication receivers in the two-dimensional coordinate system. Each transmitter can transmit a maximum of 100 W power during each radar pulse whereas the minimum allowed power for each transmitter is 1 W. Moreover, the maximum total allowable transmit power from the distributed JRC MIMO system, $P_{\text{total}_{\max}}$, is 400 W. The data rate for the communication system is calculated in terms of Shannon's capacity.

The magnitude of all elements of the RCS vector $\mathbf{h}$ is assumed to be uniformly distributed between 0.9 to 1. For this simulation, we took the magnitude of $\mathbf{h}$ as [0:962; 0:912; 0:969; 0:977; 0:907; 0:918; 0:945; 0:952; 0:982; 0:957; 0:946; 0:945; 0:952; 0:982; 0:957; 0:964; 0:941; 0:915; 0:956; 0:909; 0:906; 0:979; 0:980; 0:996; 0:902]$^T$ whereas their phases independently follow the uniform distribution. The path loss coe cients $_{m;n}$ and $_{m;r}$ are calculated using the location coordinates of the distributed JRC MIMO system, the communication receivers, and the target, whereas $_m$ = 8:773 $10^5$ is assumed for all 1 $m$ $M$. For the communication purpose, we considered $_1$ = [1=0:8; 1=1; 1=0:01; 1=0:9; 1=0:95]$^T$ and $_2$ = [1=0:6; 1=0:9; 1=0:01; 1=0:85; 1=0:73]$^T$. In this case, both communication receivers experience deep fading with the third transmitter of the distributed JRC MIMO system. On the other hand, the path loss coe cients $_{m;n}$ are the highest for the third transmitter of the JRC system because of its proximity with the target. This implies that the third transmitter is the most important in determining the target localization. However, it is the least important for optimizing the data rate for the communication system due to the smallest communication SNR (deep fading) with both communication receivers.

Table 3.1 summarizes the power allocation results and the radar as well as communication performance for the optimization strategies of the radar-only case [52], the communication-only case, and the proposed JRC case. The desired radar performance is the mean squared localization error of $_{\text{desired}}$ = 10 m$^2$.

The radar-only optimization scheme described in (3.7) provides the optimal power required for the acceptable operation of radar. It allocates most of the transmit power to the third transmitter because it provides the best target localization accuracy due to its lowest path loss coe cient. However, the third transmitter has poor communication channel conditions, thus making it unsuitable for joint radar-communication operation because the yielding communication sum data rate is only 8.87 bits/pulse.

Table 3.1: Power allocation for proposed JRC system for $M = N = 5$ and $R = 2$, $P_{\text{total}_{\max}} = 400$ W, $_{\text{desired}} = 10$ m$^2$

| | Radar-only (3.7) | Communication-only (3.9) | JRC (3.10) |
|---|---|---|---|
| $p_{tx}$ (W) | $\begin{bmatrix} 1{:}0 \\ 1{:}0 \\ 90{:}46 \\ 1{:}0 \\ 1{:}0 \end{bmatrix}$ | $\begin{bmatrix} 99{:}45 \\ 99{:}95 \\ 1{:}02 \\ 99{:}86 \\ 99{:}72 \end{bmatrix}$ | $\begin{bmatrix} 89{:}39 \\ 81{:}27 \\ 72{:}22 \\ 79{:}43 \\ 77{:}69 \end{bmatrix}$ |
| $P_{\text{total}}$ (W) | 94:46 | 400 | 400 |
| ($m^2$) | 9:97 | 30:59 | 8:21 |
| < (bits/pulse) | 8:87 | 51:16 | 50:44 |

The communication-only scheme (3.9) exploits water- lling under the available power constraint to achieve the optimal sum data rate of 51.16 bits/pulse. It can be observed that the least power is allocated to the third transmitter due to its worst communication conditions and more power is allocated to other transmitters with better communication channel conditions. Although this scheme is the best to achieve the optimal data rate, it results in a high CRB of = 30:59 m$^2$ while using 400 W power, thus failing to achieve the desired radar performance, even consuming the maximum allowable total power.

The distributed JRC MIMO scheme described in (3.10) allocates the optimal power to di erent transmitters by simultaneously considering the communication and radar objectives. As the radar objective is the primary one, it is observed that the JRC scheme allocates a considerable amount of power to the third transmitter, resulting in the desired target localization accuracy with = 8:21 m$^2$, whereas the secondary communication operation achieves a sum data rate of 50:44 bits/pulse. The results clearly con rm the promising performance of the proposed strategy.

## 3.5 Remarks

In this chapter, we proposed a distributed JRC MIMO system which optimizes the power allocation for a desired localization accuracy of the radar and improves the communication data rate by considering the channel side information. The power allocation was derived for the maximum allowable total power of the JRC transmitters ensuring the desired radar-communication performance. Simulation results verify the e ectiveness of the proposed scheme.

# Chapter 4

# Future Direction: Sensor Selection Strategies for JRC System

In this section, we discuss sensor selection strategies for beamforming based JRC systems. Optimal sensor selection is anticipated as an attractive means to achieve superior performance with a low hardware cost because of the ever-decreasing cost of the sensor deployment compared to the radio frequency (RF) chains and processors. We address optimal sensor selection by exploiting a constrained re-weighted $\ell_1$-norm minimization with low computational complexity. For the future work, we will argue that the group sparsity based sensor selection eases the hardware implementation by mollifying the unnecessary sensor switching and enables effective utilization of up-conversion chains.

## 4.1 Sensor Selection for Beamforming Based JRC Systems

In practical systems, there are usually more sensors than the expensive radio transmission chains. Ideally, it is desirable to automatically switch the available chains to the most appropriate subset of sensors which provides the best performance for

the whole system, especially in an adaptive fashion. Each radio transmission chain consists of a digital-to-analog converter, a mixer, and a power amplifier. On the other hand, transmit sensors are not only becoming cheaper but also getting smaller in size. Therefore, optimal sensor selection has crucial importance in the modern systems. A lot of research efforts have been invested in this direction in context of several applications in communications and radar systems [39, 44, 53, 55–61]. These efforts mostly focus on the optimal sensor selection and effective power allocation in colocated as well as distributed sensor systems.

Optimal sensor selection for JRC systems has been discussed for sensor arrays as well as the distributed systems. In [39] and [61], sparse array optimization has been performed to extract the sensor array geometries ideal for the JRC system operation. The sensor array degrees-of-freedom in such systems are exploited to suppress the cross-interference of the systems and improve the communication data rate. On the other hand, [44] addresses the power allocation and sensor selection for distributed JRC system based on the nature of the target's radar cross-section and the quality of communication channels. The basic principle of sensor selection strategies for beamforming based JRC systems is illustrated in Fig. 4.1.

We will focus on selection strategies inspired by re-weighter $l_1$ norm minimization discussed in [62]. We are still working in this research direction; however, the preliminary simulation results are presented.

Consider a JRC system consisting of an $M$-element transmit linear array. The JRC system exploits different beamforming weight vectors over time to transmit different communication information towards the communication receivers while all beamforming vectors offer similar radar mainlobe patterns. The vector $\mathbf{a}(\ ) = [e^{j2\ d_1 \sin(\ )=\ }; : : : ; e^{j2\ d_M \sin(\ )=\ }]^T$ represents the array manifold where $d_m$ is the location of the $m$th sensor ($1 \quad m \quad M$) and is the signal wavelength. The radar surveillance region, sidelobe region, and the transition region are respectively denoted

by $_{rad}$, $_{sl}$, and $_{trans}$. We consider $C$ communication users located within the sidelobe region of the radar, and the angular direction of the $c$th user ($1 \quad c \quad C$) is $_c$, where $_c \; 2 \quad _{com} \quad _{sl}$. The JRC system exploits $N$ beamforming weight vectors where the vector $\mathbf{w}_n$ ($1 \quad n \quad N$) satisfying the radar and communication objectives can be obtained from the following optimization [38]:

$$\begin{aligned} &\min_{\mathbf{w}_n} \max_{r} \; G_{\text{rad}} e^{j\,'(\,r)} \quad \mathbf{w}_n^{\text{H}} \mathbf{a}(\,_r) \;; \qquad _r \; 2 \quad _{\text{rad}}; \\ &\text{subject to} \quad \mathbf{w}_n^{\text{H}} \mathbf{a}(\,_{"}) \quad "_{\text{sl}}; \qquad\qquad _{"} \; 2 \quad _{\text{sl}}; \\ &\qquad\qquad \mathbf{w}_n^{\text{H}} \mathbf{a}(\,_c) = e^{j\,_{n;c}} \quad _{n;c}; \qquad 1 \quad c \quad C; \end{aligned} \tag{4.1}$$

where $G_{\text{rad}}$ is the desired beamforming gain in the mainlobe region, $'(\,)$ denotes the corresponding desired phase pro le, and $"_{\text{sl}}$ is the maximum allowable sidelobe amplitude level. The distinct gains and phases associated with the direction of communication user $c$, respectively denoted as $_{n;c}$ and $e^{j\,_{n;c}}$, represent the transmitted communication information towards that user. Note that this scheme enables multiple access by using distinct amplitudes and phases, as embedded in a QAM symbol, towards di erent communication receivers [38]. Note that, in order to use $L$ amplitudes and $Q$ phases towards each communication receiver, the JRC system requires $N = (LQ)^C$ unique beamforming weight vectors.

The JRC system exploits $K$ dual-purpose waveforms which are utilized for both radar and communication operations are the same. These waveforms $_1(t); \; _2(t); \; : : : ; \; _K(t)$ satisfy the following orthogonality property:

$$\frac{1}{T} \int_0^T \; _{k_1}(t) \quad _{k_2}(\,)\mathrm{d}t = \quad (k_1 \quad k_2) \quad (t \quad ); \tag{4.2}$$

where $1 \quad k_1; k_2 \quad K$ are positive integers, $t$ is the fast time[1], $T$ denotes the time duration of each radar pulse, $_{k_2}(\,)$ represents the time-delayed version of $_{k_2}(t)$ delayed by time $t(< T)$, and $(\,)$ is the Kronecker delta function.

[1]see Section A.2.1 of Appendix A for detail on fast time

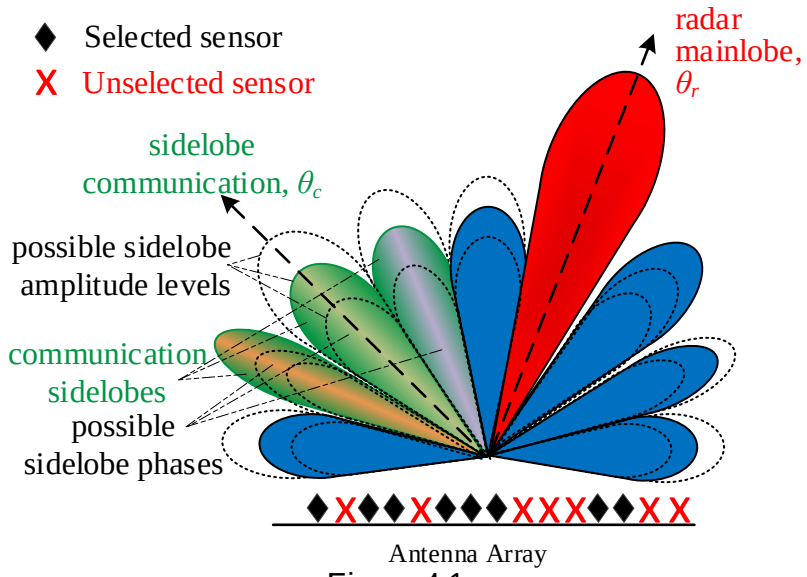


Figure 4.1: .
Sensor selection for JRC system (`x' denotes unselected sensor positions).

For the $n$th beamforming vector, the transmit signal from the JRC sensor array takes the following form:

$$x(t) = w_{n\ k}(t): \tag{4.3}$$

The beamforming vector $w_n$ satis es the radar mainlobe gain objective and projects the QAM symbols of amplitude $_{n;c}$ and phase $e^{j\ _{n;c}}$ towards the $c$th communication user with waveform $_k(t)$. The JRC system can vary the transmitted communication information by exploiting di erent beamforming weight vectors and the corresponding waveforms over the course of time [38].

## 4.2 Sensor Selection Strategies

We will work on two sensor selection strategies for transmit beamforming-based JRC system. In both strategies, the JRC system optimizes the beamforming weight vectors such that the number of selected sensors and the transmit power is minimized. Since these objectives may be con icting, more emphasis is given to the sensor selection objective. The main idea of JRC system with sensor selection is illustrated in Fig. 4.1. The basic principle of both strategies is expressed as follows:

In the first scheme, the sensors are separately selected for each individual beamforming weight vector. Although this scheme works well in theory, it renders frequency sensor switching when different beamforming weight vectors are associated with different sensor selection patterns. In addition, this generally requires more sensors to be activated (as the union of all sensor selection patterns).

In the second scheme, we will investigate a joint sensor selection strategy while extracting multiple beamforming weight vectors concurrently. As such, this approach avoids sensor switching, leading to a simpler and more practical hardware design. Since all beamformers will use the same set of selected sensors, it provides effective sensor utilization compared to the first strategy.

The details of these two approaches are respectively discussed in the following two subsections. We will also present the preliminary results for the first approach.

### 4.2.1 Sensor Selection for Individual Beamformers

We minimize the total number of active sensors as well as the total transmit power of the JRC system through the following multi-objective optimization:

$$\begin{aligned} \min_{\mathbf{w}_n} \quad & \|\mathbf{w}_n\|_2^2 + \|\mathbf{w}_n\|_0 \\ \text{s.t.} \quad & |G_{\text{rad}} e^{j\psi(\theta_r)} - \mathbf{w}_n^H \mathbf{a}(\theta_r)| \le \varepsilon_{\text{tol}}, \quad \theta_r \in \Theta_{\text{rad}}, \\ & |\mathbf{w}_n^H \mathbf{a}(\theta_s)| \le \varepsilon_{\text{sl}}, \quad \theta_s \in \Theta_{\text{sl}}, \\ & \mathbf{w}_n^H \mathbf{a}(\theta_c) = \alpha_{n,c} e^{j\phi_{n,c}}, \quad c = 1, \ldots, C. \end{aligned} \tag{4.4}$$

Here, $\rho$ is the tuning parameter which trades off between the two objectives, and $\varepsilon_{\text{tol}}$ is the maximum bearable tolerance for the radar mainlobe. The $\ell_0$-norm-based nonconvex objective tries to minimize the number of selected sensors and $\ell_2$-norm-based objective tends to minimize the total transmit power. The $\ell_0$-norm in (4.4) can

be relaxed by exploiting the $\ell_1$-norm, albeit a weaker and indirect measure of sparsity [62], resulting in the following optimization:

$$\begin{aligned} \min_{\mathbf{w}_n} \quad & \|\mathbf{w}_n\|_2^2 + \|\mathbf{w}_n\|_1 \\ \text{s.t.} \quad & |G_{\text{rad}} e^{j\psi(\theta_r)} - \mathbf{w}_n^{\mathsf{H}} \mathbf{a}(\theta_r)| \le \epsilon_{\text{tol}}, \quad \theta_r \in \Theta_{\text{rad}}, \\ & |\mathbf{w}_n^{\mathsf{H}} \mathbf{a}(\theta_{\text{sl}})| \le \epsilon_{\text{sl}}, \quad \theta_{\text{sl}} \in \Theta_{\text{sl}}, \\ & \mathbf{w}_n^{\mathsf{H}} \mathbf{a}(\theta_c) = \alpha_{n,c} e^{j\phi_{n,c}}, \quad c = 1, \ldots, C. \end{aligned} \tag{4.5}$$

While the optimization (4.5) enforces sparsity in the beamforming weight vector $\mathbf{w}_n$ by exploiting the $\ell_1$-norm, the sensors with a higher beamforming gain are penalized more compared to those with a lower beamforming gain, thus yielding a sub-optimal sparsity solution. This issue can be mitigated by introducing a re-weighting function in the $\ell_1$-norm-based objective function (4.5) to enforce the sparsity in a democratic way as follows:

$$\begin{aligned} \min_{\mathbf{w}_n} \quad & \|\mathbf{w}_n\|_2^2 + \|\mathbf{u}_n^{(i)} \mathbf{w}_n\|_1 \\ \text{s.t.} \quad & |G_{\text{rad}} e^{j\psi(\theta_r)} - \mathbf{w}_n^{\mathsf{H}} \mathbf{a}(\theta_r)| \le \epsilon_{\text{tol}}, \quad \theta_r \in \Theta_{\text{rad}}, \\ & |\mathbf{w}_n^{\mathsf{H}} \mathbf{a}(\theta_{\text{sl}})| \le \epsilon_{\text{sl}}, \quad \theta_{\text{sl}} \in \Theta_{\text{sl}}, \\ & \mathbf{w}_n^{\mathsf{H}} \mathbf{a}(\theta_c) = \alpha_{n,c} e^{j\phi_{n,c}}, \quad c = 1, \ldots, C, \end{aligned} \tag{4.6}$$

where the $m$th element of the weighting function $\mathbf{u}_n$ is expressed as [62]:

$$u_{n,m} = \begin{cases} \dfrac{1}{|w_{n,m}|}, & \text{if } |w_{n,m}| > 0, \\ 1/\varepsilon, & \text{if } |w_{n,m}| = 0. \end{cases} \tag{4.7}$$

Here, $w_{n,m}$ is the $m$th element of $\mathbf{w}_n$, and $\varepsilon$ should be set slightly smaller than the expected nonzero magnitudes of $\mathbf{w}_n$. The optimization (4.6) is executed in an iterative manner such that the coefficients $\mathbf{u}_n^{(i+1)}$ are updated using the beamforming weights $\mathbf{w}_n$ after the $i$-th iteration. For the first iteration, $\mathbf{u}_n^{(1)} = \mathbf{1}_{M \times 1}$. The solution of

such iterative $\ell_1$-norm-based optimization is closer to the $\ell_0$-norm-based counterpart within few (2{15) iterations [62].

### 4.2.2 Group sparsity-based Joint Sensor Selection for Multiple Beamformers

As we discussed above, the optimization (4.6) for di erent individual beamforming weight vectors may result in di erent sets of selected sensors. This is highly undesirable because the required frequent sensor switching introduces unnecessary complexity in hardware implementation. Moreover, all the beamforming weight vectors collectively use a higher number of sensors even each individual beamforming weight vector exploits very few sensors.

We propose a joint optimal sensor selection strategy which minimizes the total number of sensors used by all the beamformers for the JRC operation. For this purpose, we exploit the mixed $\ell_{1,2}$-norm-based group-sparsity concept [63]. The mixed $\ell_{1,2}$-norm is de ned as:

$$\|\mathbf{w}\|_{1,2} := \left( \sum_{m=1} \left( \sum_{n=1} |w_{n,m}|^2 \right) \right)^{0.5} : \tag{4.8}$$

The proposed multi-objective optimization for sensor selection exploits group-sparsity to extract all beamforming weight vectors and takes the following form:

$$\begin{aligned} \min_{\mathbf{w}_n} \quad & \sum_{n=1} \|\mathbf{w}_n\|_2^2 + \|\mathbf{w}\|_{1,2} \\ \text{s.t.} \quad & |G_{\text{rad}} e^{j\varphi(\theta_r)} - \mathbf{w}_n^H \mathbf{a}(\theta_r)| \le \text{tol}, \quad \theta_r \in \Theta_{\text{rad}}, \\ & |\mathbf{w}_n^H \mathbf{a}(\theta_{\text{sl}})| \le \varepsilon_{\text{sl}}, \quad \theta_{\text{sl}} \in \Theta_{\text{sl}}, \\ & \mathbf{w}_n^H \mathbf{a}(\theta_c) = \rho_{n,c} e^{j\psi_{n,c}}, \quad c = 1, \ldots, C. \end{aligned} \tag{4.9}$$

Note that, contrary to the optimization (4.6) which is exploited for each beamforming weight vector separately, the optimization (4.9) jointly solves all $N$ beamforming vectors simultaneously. The mixed $\ell_{1,2}$-norm enforces the group sparsity, resulting in the selection of exactly the same sensors for all the beamforming weight vectors. However, each beamforming weight vector will have unique weights depending on its radar and communication requirements.

Similar to the weighting function in Eq. (4.7), the group sparsity in optimization (4.9) can also be enhanced democratically by exploiting a similar weighting function as follows:

$$v_m = \begin{cases} \left( \sum_{n=1}^{N} |w_{n,m}|^2 \right)^{-0.5}, & \text{if } \sum_{n=1}^{N} |w_{n,m}|^2 > 0, \\ 1/\varepsilon, & \text{if } \sum_{n=1}^{N} |w_{n,m}|^2 = 0, \end{cases} \tag{4.10}$$

where $v_m$ denotes the weight for the $m$th sensor. The resulting group sparsity-based optimization jointly produces all $N$ beamforming weight vectors as:

$$\begin{aligned} \min_{\mathbf{w}_n} \quad & \sum_{n=1}^{N} \|\mathbf{w}_n\|_2^2 + \mu \left\| \mathbf{v}^{(i)} \mathbf{W} \right\|_{1,2} \\ \text{s.t.} \quad & |G_{\text{rad}} e^{j\phi(\theta_r)} - \mathbf{w}_n^H \mathbf{a}(\theta_r)| \le \text{tol}, \quad \theta_r \in \Theta_{\text{rad}}, \\ & |\mathbf{w}_n^H \mathbf{a}(\theta_\ell)| \le \varepsilon_{\text{sl}}, \quad \theta_\ell \in \Theta_{\text{sl}}, \\ & \mathbf{w}_n^H \mathbf{a}(\theta_c) = \alpha_{n,c} e^{j\beta_{n,c}}, \quad c = 1, \ldots, C. \end{aligned} \tag{4.11}$$

where $\mathbf{v}^{(i)}$ denotes the weighting function obtained in the $i$th iteration and

$$\left\| \mathbf{v} \mathbf{W} \right\|_{1,2} = \sum_{m=1}^{M} \left( \sum_{n=1}^{N} |v_m w_{n,m}|^2 \right)^{0.5} = \sum_{m=1}^{M} v_m \left( \sum_{n=1}^{N} |w_{n,m}|^2 \right)^{0.5}. \tag{4.12}$$

Eq. (4.11) is solved in an iterative fashion until the convergence is achieved. This multi-objective optimization tends to select the array sensors that are shared by all beamforming weight vectors and minimize the total transmit power.

## 4.3 Preliminary Results

In this section, we present simulation results to illustrate the performance of the selection strategy for the individual beamforming weight vectors. The simulation results for the group sparsity based sensor selection will be provided later.

In the simulations, we consider a ULA consisting of $M = 30$ transmit sensors to optimize the radar mainlobe objectives and serve two ($C = 2$) communication users located in the sidelobe region of the radar at angles $30^o$ and $40^o$, respectively. We set the inter-sensor spacing of the ULA at 0:5 and the tuning coe cient for all the multi-objective optimizations is set to unity. The maximum allowable sidelobe level for all the cases is considered to be lower than $"_{sl} = 20$ dB.

We use the open-source SDPT3 solver [49, 50] integrated with the open-source version of CVX toolbox [47, 48] to solve all the optimizations.

For the simulation involving the focused beampattern, the JRC radar objective is to focus the main beam with a gain of 0 dB at $_r = 0^o$. For at-top beampattern synthesis experiment, the radar objective is to project the main beam with a gain of 0 dB for angles from $7^o$ to $7^o$. For this purpose, we consider $_{sl}$ consisting of a grid of angles with a grid spacing of $1^o$.

### 4.3.1 Individual Beampattern Synthesis

First, we consider the beampattern synthesis for the radar main beam focused at $_r = 0^o$. In this scenario, the JRC system aims to project an amplitude of 20 dB towards the both communication receivers. Fig. 4.2(a) demonstrates the power distribution pro le of the beamforming weight vector extracted using the optimization (4.6). The corresponding number of selected sensors during each iteration is illustrated in Fig. 4.2(b). Moreover, Fig. 4.2(c) shows the spatial selection pro le during each iteration for the rst 12 iterations. It can be observed that the algorithm converges very

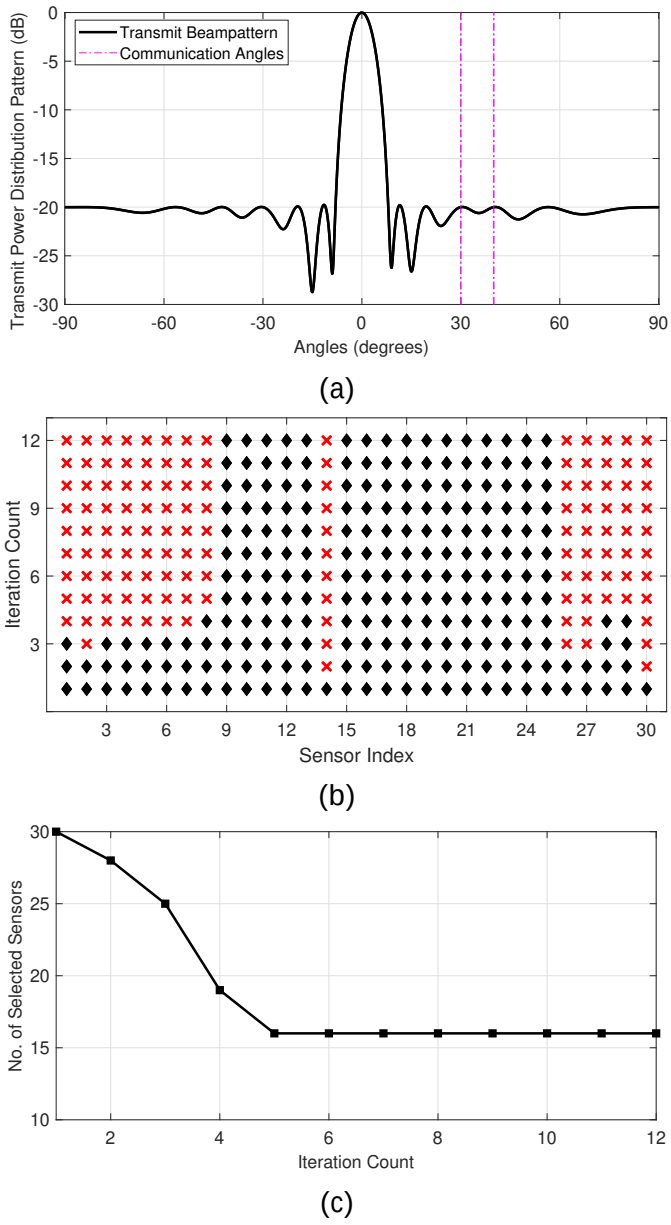


Figure 4.2: Focused beampattern synthesis using the optimal sensor selection strategy: (a) Transmit power distribution pattern, (b) Spatial sensor selection pro le for each iteration, (c) Total number of selected sensors w.r.t the number of iterations.

fast, i.e. only 5 iterations were enough to achieve the nal solution. It can also be observed that the spatial pro le of the selected sensors does not change after the convergence. From Fig. 4.2(c), note that the resulting solution did not de-select any of the sensors after the rst iteration; however, the re-weighted $l_1$-norm based optimization signi cantly enhanced the sparsity later on. Moreover, we also ran the

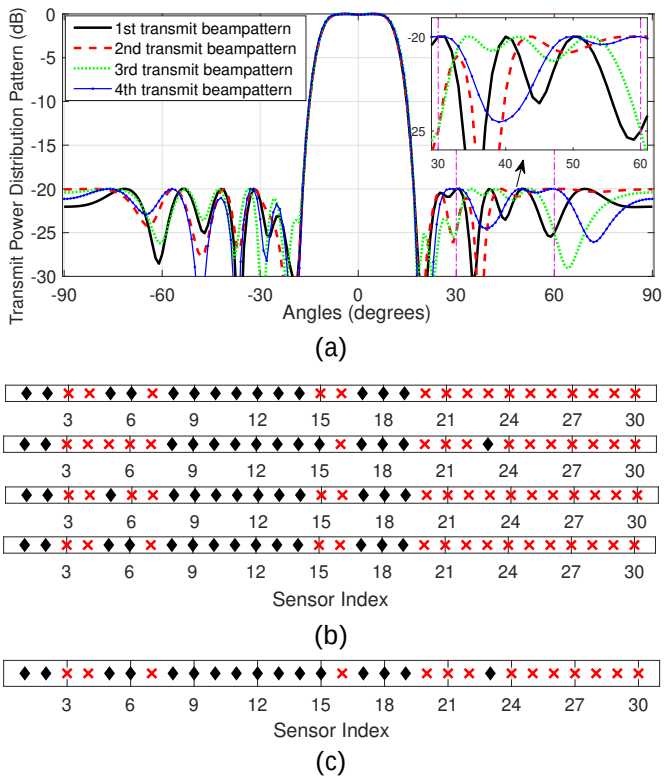


Figure 4.3: Flat-top beampattern synthesis for the proposed sensor selection strategy: (a) Transmit power pattern, (b) Final sensor selection pro le for each beampattern, (c) Overall sensor selection pro le containing sensors selected by all beamforming weight vectors.

algorithm for up to 100 iterations but did not observe any change in the spatial sensor selection pro le.

In the second example, we discuss the performance of sensor selection strategy for individual beamforming weight vectors for the case of at-top radar transmit beampattern. We also consider BPSK signaling for communication users where the JRC transmit array has an objective to transmit two di erent amplitude levels of 20 dB and 25 dB towards both communication receivers, resulting in four di erent beamforming weight vectors.

For this simulation, we individually synthesized the four beamforming weight vectors through (4.6), and the beampatterns are illustrated in Fig. 4.3(a). The nal sensor selection pro le for these respective beamformers is shown in Fig. 4.3(b). It is

observed that these beamforming weight vectors respectively use 14, 14, 13, and 14 sensors. As a result, overall 16 sensors are needed, as depicted in Fig. 4.3(c). For large number of beamforming vectors, such di erence in the selected sensors corresponding to each beamforming vector will require a high number of sensors, thus inviting frequent sensor switching, a high hardware complexity, and sub-optimal sensor utilization.

## 4.4 Future Work

The research work will be continued in the direction of sensor selection strategies for JRC systems. In this context, we will accomplish the goals related to the group sparsity based sensor selection. Moreover, we will also continue the work in direction of spectrum sensing and over-the-horizon radar. Our objective will be to submit the achieved results for publication in *IEEE Transactions on Aerospace & Electronic Systems*, *IEEE Transactions on Signal Processing* or a similar impact journal. The future timeline for 2020 is illustrated in Table 4.1.

Table 4.1: Timeline for year 2020

| | Jan.-Mar. | | Apr.-Jun. | | Jul.-Aug. | | Sep.-Oct. | | Nov.-Dec. |
|---|---|---|---|---|---|---|---|---|---|
| Sensor selection for JRC | ✓ | ✓ | ✓ | | | | | | |
| Compile dissertation | | | ✓ | ✓ | ✓ | | | | |
| Review circulate dissertation | | | | | | ✓ | | | |
| Announce defense | | | | | | | ✓ | | |
| Dissertation defense | | | | | | | | ✓ | |
| Address panel concerns | | | | | | | | ✓ | ✓ |
| Submit dissertation | | | | | | | | | ✓ |
| Compile publications | ✓ | ✓ | ✓ | ✓ | ✓ | ✓ | ✓ | | |
| Respond to reviewers | ✓ | ✓ | ✓ | ✓ | ✓ | ✓ | ✓ | ✓ | ✓ |

# Bibliography


[1] H. Gri ths, S. Blunt, L. Cohen, and L. Savy, \Challenge problems in spectrum engineering and waveform diversity," in *Proc. IEEE Radar Conf.*, Ottawa, Canada, Apr.{May 2013, pp. 1{5.

[2] H. Gri ths, L. Cohen, S. Watts, E. Mokole, C. Baker, M. Wicks, and S. Blunt, \Radar spectrum engineering and management: Technical and regulatory issues," *Proc. IEEE*, vol. 103, no. 1, pp. 85{102, Jan. 2015.

[3] C. Baylis, M. Fellows, L. Cohen, and R. J. Marks, \Solving the spectrum crisis: Intelligent, recon gurable microwave transmitter ampli ers for cognitive radar," *IEEE Microw. Mag.*, vol. 15, no. 5, pp. 94{107, July-Aug. 2014.

[4] H. T. Hayvaci and B. Tavli, \Spectrum sharing in radar and wireless communication systems: A review," in *Proc. Int. Conf. Electromagn. in Advanced Appl.*, Palm Beach, Aruba, Aug. 2014, pp. 810{813.

[5] S. Kumar, G. Costa, S. Kant, B. F. Flemming, N. Marchetti, and P. Mogensen, \Spectrum sharing for next generation wireless communication networks," in *Proc. First Int. Workshop on Cognitive Radio and Advanced Spectr. Manag.*, Aalborg, Denmark, Feb 2008, pp. 1{5.

[6] E. Biglieri, *Principles of Cognitive Radio*. Cambridge University Press, 2012.

[7] Z. Geng, H. Deng, and B. Himed, \Adaptive radar beamforming for interference mitigation in radar-wireless spectrum sharing," *IEEE Signal Process. Lett.*, vol. 22, no. 4, pp. 484{488, apr 2015.

[8] Kuan-Wen Huang, M. Bica, U. Mitra, and V. Koivunen, \Radar waveform design in spectrum sharing environment: Coexistence and cognition," in *Proc. IEEE Radar Conf.*, Johannesburg, South Africa, May 2015, pp. 1698{1703.

[9] B. Li and A. P. Petropulu, \Joint transmit designs for coexistence of MIMO wireless communications and sparse sensing radars in clutter," *IEEE Trans. Aerosp. Electron. Syst.*, vol. 53, no. 6, pp. 2846{2864, Dec 2017.

[10] B. Li, A. P. Petropulu, and W. Trappe, \Optimum co-design for spectrum sharing between matrix completion based MIMO radars and a MIMO communication system," *IEEE Trans. Signal Process.*, vol. 64, no. 17, pp. 4562{4575, Sept 2016.

[11] A. Khawar, A. Abdelhadi, and T. C. Clancy, \Coexistence analysis between radar and cellular system in los channel," *IEEE Antennas Wireless Propag. Lett.*, vol. 15, pp. 972{975, 2016.

[12] J. A. Mahal, A. Khawar, A. Abdelhadi, and T. C. Clancy, \Spectral coexistence of MIMO radar and MIMO cellular system," *IEEE Trans. Aerosp. Electron. Syst*, vol. 53, no. 2, pp. 655{668, April 2017.

[13] D. W. Bliss, \Cooperative radar and communications signaling: The estimation and information theory odd couple," in *Proc. IEEE Radar Conf.*, Cincinnati, OH, May 2014, pp. 50{55.

[14] F. Paisana, N. Marchetti, and L. A. DaSilva, \Radar, TV and cellular bands: Which spectrum access techniques for which bands?" *Commun. Surveys & Tuts.*, vol. 16, no. 3, pp. 1193{1220, 2014.

[15] F. Liu, C. Masouros, A. Li, and T. Ratnarajah, \Robust MIMO beamforming for cellular and radar coexistence," *IEEE Wireless Commun. Lett.*, vol. 6, no. 3, pp. 374{377, June 2017.

[16] S. C. Surender, R. M. Narayanan, and C. R. Das, \Performance analysis of communications & radar coexistence in a covert UWB OSA system," in *Proc. IEEE Global Telecommunications Conf.*, Miami, FL, Dec. 2010, pp. 1{5.

[17] C. Sturm, T. Zwick, and W. Wiesbeck, \An OFDM system concept for joint radar and communications operations," in *Proc. IEEE 69th Veh. Technol. Conf.*, Barcelona, Spain, April 2009, pp. 1{5.

[18] S. D. Blunt, M. R. Cook, and J. Stiles, \Embedding information into radar emissions via waveform implementation," in *International Waveform Diversity and Design Conf.*, Niagara Falls, Canada, Aug. 2010, pp. 195{199.

[19] A. Hassanien, M. G. Amin, Y. D. Zhang, and F. Ahmad, \Signaling strategies for dual-function radar communications: an overview," *IEEE Aerosp. Electron. Syst. Mag.*, vol. 31, no. 10, pp. 36{45, Oct. 2016.

[20] J. Euziere, R. Guinvarc'h, M. Lesturgie, B. Uguen, and R. Gillard, \Dual function radar communication time-modulated array," in *Proc. International Radar Conf.*, Lille, France, Oct. 2014, pp. 1{4.

[21] A. Hassanien, M. G. Amin, Y. D. Zhang, and F. Ahmad, \A dual function radar-communications system using sidelobe control and waveform diversity," in *Proc. IEEE Radar Conf.*, Arlington, VA, May 2015, pp. 1260{1263.

[22] | | , \Dual-function radar-communications: Information embedding using sidelobe control and waveform diversity," *IEEE Trans. Signal Process.*, vol. 64, no. 8, pp. 2168{2181, April 2016.

[23] | |, \E cient sidelobe ASK based dual-function radar-communications," in *Proc. SPIE Defense + Security, Radar Sensor Technology Conf.*, Baltimore, MD, Apr. 2016.

[24] | |, \Dual-function radar-communications using phase-rotational invariance," in *Proc. 23rd European Signal Process. Conf.*, Nice, France, Aug. 2015, pp. 1346{1350.

[25] A. Hassanien, M. G. Amin, Y. D. Zhang, F. Ahmad, and B. Himed, \Non-coherent PSK-based dual-function radar-communication systems," in *Proc. IEEE Radar Conf.*, Philadelphia, PA, May 2016, pp. 1{6.

[26] A. Hassanien, M. G. Amin, Y. D. Zhang, and F. Ahmad, \Phase-modulation based dual-function radar-communications," *IET Radar, Sonar & Navigation*, vol. 10, no. 8, pp. 1411{1421, 2016.

[27] A. Hassanien, B. Himed, and B. D. Rigling, \A dual-function MIMO radar-communications system using frequency-hopping waveforms," in *Proc. IEEE Radar Conf.*, Seattle, WA, May 2017, pp. 1721{1725.

[28] A. Hassanien, M. G. Amin, and Y. D. Zhang, \Computationally e cient beampattern synthesis for dual-function radar-communications," in *Proc. SPIE Defense + Security, Radar Sensor Technology Conf.*, Baltimore, MD, Apr. 2016.

[29] P. M. McCormick, S. D. Blunt, and J. G. Metcalf, \Simultaneous radar and communications emissions from a common aperture, part i: Theory," in *IEEE Radar Conf.*, May 2017, pp. 1685{1690.

[30] A. R. Chiriyath, B. Paul, and D. W. Bliss, \Radar-communications convergence: Coexistence, cooperation, and co-design," *IEEE Trans. Cogn. Commun. Netw.*, vol. 3, no. 1, pp. 1{12, March 2017.

[31] A. Ahmed, Y. D. Zhang, and B. Himed, \Multi-User Dual-Function Radar-Communications Exploiting Sidelobe Control and Waveform Diversity," in *Proc. IEEE Radar Conf.*, Oklahoma City, OK., Apr. Apr. 2018.

[32] H. Deng and B. Himed, \Interference Mitigation Processing for Spectrum-Sharing Between Radar and Wireless Communications Systems," *IEEE Trans. on Aerosp. Electron. Syst.*, vol. 49, no. 3, pp. 1911{1919, July 2013.

[33] J. R. Guerci, R. M. Guerci, A. Lackpour, and D. Moskowitz, \Joint design and operation of shared spectrum access for radar and communications," in *Proc. IEEE Radar Conf.*, Arlington, VA, May 2015, pp. 0761{0766.

[34] K. W. Huang, M. Bica, U. Mitra, and V. Koivunen, \Radar waveform design in spectrum sharing environment: coexistence and cognition," in *Proc. IEEE Radar Conf.*, Arlington, VA, May 2015, pp. 1698{1703.

[35] I. P. Eedara, A. Hassanien, M. G. Amin, and B. D. Rigling, \Ambiguity function analysis for dual-function radar communications using PSK signaling," in *Proc. Asilomar Conf. Signals, Systems, and Computers*, Oct. 2018, pp. 900{904.

[36] F. Liu, L. Zhou, C. Masouros, A. Li, W. Luo, and A. Petropulu, \Toward dual-functional radar-communication systems: Optimal waveform design," *IEEE Trans. Signal Process.*, vol. 66, no. 16, pp. 4264{4279, Aug. 2018.

[37] A. Ahmed, Y. Gu, D. Silage, and Y. D. Zhang, \Power-e cient multi-user dual-function radar-communication," in *Proc. IEEE Int. Workshop Signal Process. Advances in Wireless Commun.*, Kalamata, Greece, June 2018, pp. 1{5.

[38] A. Ahmed, Y. D. Zhang, and Y. Gu, \Dual-function radar-communications using QAM-based sidelobe modulation," *Digital Signal Process.*, vol. 82, pp. 166{174, Nov. 2018.

[39] X. Wang, A. Hassanien, and M. G. Amin, \Sparse transmit array design for dual-function radar communications by antenna selection," *Digital Signal Process.*, vol. 83, pp. 223{234, Dec. 2018.

[40] S. D. Blunt, J. G. Metcalf, C. R. Biggs, and E. Perrins, \Performance characteristics and metrics for intra-pulse radar-embedded communication," *IEEE J. Sel. Areas in Commun.*, vol. 29, no. 10, pp. 2057{2066, Dec. 2011.

[41] Y. Liu, G. Liao, J. Xu, Z. Yang, and Y. Zhang, \Adaptive OFDM integrated radar and communications waveform design based on information theory," *IEEE Commun. Lett.*, vol. 21, no. 10, pp. 2174{2177, Oct. 2017.

[42] M. Bica and V. Koivunen, \Radar waveform optimization for target parameter estimation in cooperative radar-communications systems," *IEEE Trans. Aerosp. Electron. Syst.*, (in press).

[43] | | , \Multicarrier radar-communications waveform design for RF convergence and coexistence," in *Proc. IEEE Int. Conf. Acoust., Speech, Signal Process.*, Brighton, U.K., May 2019, pp. 7780{7784.

[44] A. Ahmed, Y. D. Zhang, and B. Himed, \Distributed dual-function radar-communication MIMO system with optimized resource allocation," in *Proc. IEEE Radar Conference*, Boston, MA, Apr. 2019.

[45] A. Ahmed, S. Zhang, V. S. Amin, and Y. D. Zhang, \Spectrum sharing strategy for radio frequency based medical services," in *Proc. IEEE Signal Process. in Medicine and Biology Symp.*, Philadelphia, PA, Dec. 2019 (under review).

[46] A. Hassanien, S. A. Vorobyov, and A. Khabbazibasmenj, \Transmit radiation pattern invariance in MIMO radar with application to DOA estimation," *IEEE Signal Process. Lett.*, vol. 22, no. 10, pp. 1609{1613, Oct. 2015.

[47] CVX Research, Inc., \CVX: Matlab software for disciplined convex programming, version 2.0," http://cvxr.com/cvx, Aug. 2012.

[48] M. Grant and S. Boyd, \Graph implementations for nonsmooth convex programs," in *Recent Advances in Learning and Control*, ser. Lecture Notes in Control and Information Sciences, V. Blondel, S. Boyd, and H. Kimura, Eds. Springer-Verlag Limited, 2008, pp. 95{110.

[49] R. H. Tutuncu, K. C. Toh, and M. J. Todd, \Solving semide nite-quadratic-linear programs using SDPT3," *Math. Program.*, vol. 95, no. 2, pp. 189{217, Feb 2003.

[50] K. C. Toh, M. J. Todd, and R. H. Tutuncu, \SDPT3 | a Matlab software package for semide nite programming, version 1.3," *Optim. Methods. Softw.*, vol. 11, no. 1-4, pp. 545{581, 1999.

[51] H. Godrich, A. M. Haimovich, and R. S. Blum, \Target localization accuracy gain in MIMO radar-based systems," *IEEE Trans. Inf. Theory*, vol. 56, no. 6, pp. 2783{2803, June 2010.

[52] H. Godrich, A. P. Petropulu, and H. V. Poor, \Power allocation strategies for target localization in distributed multiple-radar architectures," *IEEE Trans. Signal Process.*, vol. 59, no. 7, pp. 3226{3240, July 2011.

[53] | | , \Sensor selection in distributed multiple-radar architectures for localization: A knapsack problem formulation," *IEEE Trans. Signal Process.*, vol. 60, no. 1, pp. 247{260, Jan 2012.

[54] A. Goldsmith, *Wireless Communications*. Cambridge University Press, 2005.

[55] O. Mehanna, N. D. Sidiropoulos, and G. B. Giannakis, \Joint multicast beamforming and antenna selection," *IEEE Trans. Signal Process.*, vol. 61, no. 10, pp. 2660{2674, May 2013.

[56] O. T. Demir and T. E. Tuncer, \Antenna selection and hybrid beamforming for simultaneous wireless information and power transfer in multi-group multicasting systems," *IEEE Trans. Wireless Commun.*, vol. 15, no. 10, pp. 6948{6962, Oct 2016.

[57] L. Blanco and M. Najar, \Sparse multiple relay selection for network beamforming with individual power constraints using semide nite relaxation," *IEEE Trans. Wireless Commun.*, vol. 15, no. 2, pp. 1206{1217, Feb 2016.

[58] G. Venkatraman, A. Tolli, M. Juntti, and L. Tran, \Multigroup multicast beamformer design for MISO-OFDM with antenna selection," *IEEE Trans. Signal Process.*, vol. 65, no. 22, pp. 5832{5847, Nov 2017.

[59] O. Tervo, L. Tran, H. Pennanen, S. Chatzinotas, B. Ottersten, and M. Juntti, \Energy-e cient multicell multigroup multicasting with joint beamforming and antenna selection," *IEEE Trans. Signal Process.*, vol. 66, no. 18, pp. 4904{4919, Sep. 2018.

[60] M. Guo, Y. D. Zhang, and T. Chen, \DOA estimation using compressed sparse array," *IEEE Trans. Signal Process.*, vol. 66, no. 15, pp. 4133{4146, Aug. 2018.

[61] X. Wang, A. Hassanien, and M. G. Amin, \Dual-function MIMO radar communications system design via sparse array optimization," *IEEE Trans. Aerosp. Electron. Syst.*, vol. 55, no. 3, pp. 1213{1226, June 2019.

[62] E. J. Candes, M. B. Wakin, and S. P. Boyd, \Enhancing sparsity by reweighted $l_1$ minimization," *Journal of Fourier Analysis and Applications*, vol. 14, no. 5, pp. 877{905, Dec. 2008.

[63] M. Yuan and Y. Lin, \Model selection and estimation in regression with grouped variables," *J. R. Stat. Soc. B.*, vol. 68, pp. 49{67, Feb. 2006.

# Appendix A

# Radar Terminology

Radar is an acronym for RAdio Detection And Ranging. In simple words, it is an object detection system that transmits electromagnetic waves and analyzes the echoes re ected from the objects. However, modern radars can perform quite a lot number of tasks apart from target detection and tracking.

## A.1 Categorization of Radars

Radars can be broadly categorized into several categories. In the following, we discuss only the most common characteristics on the basis of which the radars are usually classi ed:

### A.1.1 Illuminator

Active radars are equipped with transmitter(s) which illuminate the target. On the other hand, passive radars rely on the illuminators of opportunity, like communication networks, to perform the radar tasks.

### A.1.2 Transmission Rate

Pulsed radars emit the transmit waveforms in the forms of pulses. The time duration between the activation of two pulses is called *pulse repetition interval.* The inverse of pulse repetition interval is regarded as *pulse repetition frequency.*

Continuous wave radars transmit the radar waveforms continuously. The re ected signals from the target are inspected to perform the radar tasks.

### A.1.3 Geometry

Monostatic radars perform the transmit and receive operation at the same physical location. On the other hand, transmitters and receivers are spatially employed at di erent locations in the bistatic or multistatic radars.

## A.2 Basic Operation

The simplest radar operation can be divided into 4 steps:

The radar is transmitting an electromagnetic pulse.

The radar switches to listening mode.

The pulse is re ected by a target.

The radar receives the echoes from the transmitted pulse.

Using various properties of the received echo, the radar can extract parameters such as the range and velocity of the target

### A.2.1 Radar Cross-section

Radar cross-section is a measure of how detectable an object is by radar. A larger RCS indicates that an object is more easily detected.

All objects re ect a limited amount of radar energy back to the radar. The factors that in uence this include:

The material of which the object is made;

Size of the object relative to the radar wavelength;

Absolute size of the object;

Incident and re ected angles of the radar signals with the object;

polarization of the radar transmit signals and the signals re ected by the target.

## A.3 Radar Equation

The radar equation provides the mathematical framework for the basic radar operation. According to this equation, the receive power of the radar $P_r$ due to target echo can be represented in terms of the transmit power $P_t$ as follows:

$$P_r = \frac{P_t G^2 \ ^2}{(4\ )^3 R^4 L}: \tag{A.1}$$

Here,

$P_t$: transmit power of the radar;

$P_r$: received power at the radar from the target echo;

$G$: antenna gain;

: operating wavelength;

: target radar cross-section

$R$: range from the radar to the target;

$L$: Other losses (system, propagation.

Rearranging the radar equation we get:

$$R = \frac{P_t G^2 \ ^2}{(4\ )^3 P_r L}^{0:25} : \tag{A.2}$$

This implies that the low frequencies are preferable for long-range targets.

## A.4 Range Calculation

The *range* of the target from the radar can be determined by the time-delay of the echoed signal from the target. Mathematically,

$$R = \frac{c}{2}; \tag{A.3}$$

where $c$ is the speed of electromagnetic waves and is the time-delay of the target echo. The factor of 2 in the above equation is due to the fact that the radar signals cover the distance equal to twice the range. This is because the signals travel from the radar transmitter to the target and then from the target to their way back to the radar receiver.

### A.4.1 Range Resolution

*Range resolution* is the ability of the radar to separate the closely spaced targets. The range resolution can be mathematically expressed as:

$$\frac{cT}{2} \quad \frac{c}{2B}; \tag{A.4}$$

where $T$ is the pulse duration and $B$ is the bandwidth.

If the distance between the two targets is less than $cT$=2, the re ected signal from the both targets merge with each other. Advanced technique like pulse compression can enhance the range resolution. The above equation shows that the range resolution can be improved if the radar bandwidth is very high.

### A.4.2 Maximum Unambiguous Range

Radar is not able to discriminate between echoes from an older and the current pulse transmission. In this context, we can de ne the maximum unambiguous range as follows:

$$R_{\max} = \frac{cT_{\text{pri}}}{2} = \frac{c}{2f_{\text{prf}}}; \tag{A.5}$$

where $T_{pri}$ and $f_{prf}$ respectively represent the pulse repetition interval and pulse repetition frequency.

## A.5 Slow Time and Fast Time

Radar signals from each pulse repetition interval are sorted in memory for further processing. In this context, following two definitions are important:

> Fast time: refers to the different sampling time slots composing a pulse repetition interval. Fast time is dependent on the sampling rate of radar analog-to-digital converter.
>
> Slow time: It can be considered as the pulse repetition index. It is updated once at each pulse repetition interval.

Suppose that a radar transmits pulses with a pulse repetition interval of 1 msec. The reflected signals will be recorded by the radar receiver in the fast time. The slow time index will start from 0 and will update on each pulse. If the sampling time of radar receiver is 1 sec, it will record 1000 fast time samples corresponding to each slow time index or pulse.

# Appendix B

# Software Implementation

In this chapter, we give a brief overview of the software packages used during this thesis.

## B.1 MATLAB

MATLAB is a multi-paradigm numerical computing environment and proprietary programming language developed by MathWorks. It allows matrix manipulations, plotting of functions and data, implementation of algorithms, creation of user interfaces, and interfacing with programs written in other languages.

MATLAB has served as the main programming environment for this thesis. We have integrated other useful toolboxes and solvers with MATLAB for carrying out the simulations.

## B.2 CVX

CVX is a MATLAB based modeling system for solving convex optimizations. CVX helps the users to model their optimization in the form of MATLAB expressions.

Di erent commercial and academic solvers can also be integrated with CVX; however, CVX default repository contains SeDuMI, SDPT3, Gurobi, Mosek, and GLPK. Each solver has di erent capabilities and di erent levels of performance. For instance, SeDuMi, SDPT3, and MOSEK support all of the continuous (non-integer) models that CVX itself supports, while Gurobi is more limited, in that it does not support semide nite constraints; and GLPK is limited even further. On the other hand, Gurobi, GLPK, and MOSEK support mixed-integer optimizations, while SeDuMi and SDPT3 do not.

Gurobi and Mosek require additional academic or commercial license. Academic licenses are free to download and install on educational networks. Both of these solvers can also be used with Python.